Fuel 331 (2023) 125943

Contents lists available at ScienceDirect

Fuel

journal homepage: www.elsevier.com/locate/fuel

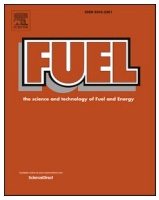

Full Length Article

Energy and exergy analysis of entrained bed gasifier/GT/Kalina cycle model for CO_2 co-gasification of waste tyre and biochar

Furkan Kartal, Uğur Özveren *

Department of Chemical Engineering, Marmara University, Goztepe Campus, 34722 Kadikoy/Istanbul, Turkey

ARTICLE INFO

Keywords:
CO_2 Co-Gasification
Kalina Cycle
IGCC
Biochar
Waste Tyre
Aspen HYSYS

ABSTRACT

Integrated gasification combined cycle (IGCC) is a power generation technology that partially oxidizes solid feedstocks to produce syngas, drives high-efficiency gas turbines (GT), recovers waste heat and uses it to generate electricity, etc. In this study, a new IGCC model for an entrained bed gasifier/GT/Kalina cycle for CO_2 co-gasification was developed for the first time using Aspen HYSYS, and an energy and exergy analysis of this model was performed to provide decision makers with a comprehensive overview of whether the energy conversion system is designed to be sustainable from a variety of perspectives. The newly proposed integrated system was used to study the CO_2/air gasification process of the biochar/waste tyre blend. Although entrained bed gasifiers have been modelled using different software and different fuels, no study on the Kalina cycle integrated biochar/waste tyre co-gasification process using Aspen HYSYS has not been reported yet. In addition, most parametric studies on integrated Kalina combined cycles focus on the influence of the Kalina cycle or a few operating factors. However, in this study, the effects of a variety of gasification process operating conditions on the performance of the combined cycle are considered.

The equivalence ratio (ER) for a high-efficiency integrated system ranged from 0.23 to 0.25, and the CO_2 content in the gasifying agent was in the range of 5–7%. While increasing the waste tyre content in the feedstock enhances H_2 production, operating the entrained bed gasifier at relatively low temperature is more efficient. Increasing the ammonia content in the working fluid also improves efficiency, and the inlet pressure of the Kalina turbine should be maintained at 28 bar to maximize performance. While the integration of the GT enables significant power generation, optimizing the operating conditions of the gasifier, which has the highest exergy dissipation, is critical to the performance of the integrated system.

1. Introduction

Energy consumption and production alternatives are key topics in several disciplines. Worldwide energy consumption is expanding due to industrialization and a growing global population. Since the industrial revolution, rising energy consumption has led to several environmental challenges such as ozone depletion, global warming, and climate change [1]. The strong dependence on fossil fuels, along with the associated price and supply chain issues, increases the need for efficient utilization of current energy sources [2]. As a consequence, in many sections of the power generation system, the more effective and suitable use of energy resources is becoming vital.

Because of its organic composition, carbon stability, and vast availability, biomass is regarded as a viable source of renewable energy and biobased technologies [3]. Its energy-producing capacity varies depending on the technology used. Encouraging energy production and secondary energy products (solid, liquid, and gaseous fuels) from forestry, industrial and agricultural residues should be promoted since it is globally accessible [4]. Biochars have received much interest in recent years due to their high carbon density and low volatile matter component [5]. Biochar is a solid material produced from the pyrolysis of biomass that has significantly better properties over the raw material used in solid fuel applications [6]. Biochar has a higher calorific value than raw biomass owing to the higher fixed carbon content. Furthermore, waste tyres are a major environmental problem owing to the fast worldwide increase in automobile ownership and the lack of both economic and technological methods. It seems reasonable to employ tyre

Abbreviations: IGCC, Integrated gasification combined cycle; ER, Equivalence ratio; SOFC, Solid oxide fuel cell; LNG, Liquefied natural gas; ad, Air dried basis; db, Dry basis; wt, Weight; GT, Gas turbine; LHV, Lower heating value.

* Corresponding author.
E-mail address: ugur.ozveren@marmara.edu.tr (U. Özveren).

https://doi.org/10.1016/j.fuel.2022.125943
Received 4 April 2022; Received in revised form 27 August 2022; Accepted 5 September 2022
Available online 13 September 2022

Nomenclature

G^t	Total Gibbs energy of a system
G_i^m	The universal standard Gibbs free energy
$\Delta G_{f,i}^m$	Standard Gibbs free energy for the formation of species i
μ_i	Chemical potential of species i
f_i	Fugacity of the i_{th} species
L	Lagrange function
λ	Lagrange multiplier
a_{ij}	The number of atoms of the j_{th} element involved in each molecule of the chemical species i
β	Ratio of chemical exergy to LHV
η	Efficiency
ε_{ph}	Physical exergy
ε_{ch}	Chemical exergy
EX_{ch}	Chemical exergy equation for a mixed gas

rubber's high energy and raw material capabilities to continue the pursuit for waste reduction/recycling, as it has a higher calorific value than coal [7]. Gasification is an excellent approach for treating biomass/biochar and waste tyres while recovering significant energy.

Gasification is the high-temperature reaction of solid fuels with an oxidant such as oxygen, air, CO_2, steam or a combination of these gases to produce syngas, which is rich in CO/H_2 [8]. Gasification is considered a reasonable clean and efficient energy production method with environmental benefits when compared to other traditional energy production systems [9]. Gasification can save energy over direct combustion, which uses excessive oxygen to combust solid fuels. Applying gasification technology can also increase thermal efficiency by 12% and reduce CO_2 emissions by 37% [10]. Syngas, which is the final gaseous product of gasification procedure, is a significant secondary fuel in the diverse industries with its applications such as being used as a primary fuel, chemical synthesis, power generation via fuel cells and GTs [11]. High-quality syngas can be produced by the gasification procedure from solid feedstock materials such as biomass, biochar, coal, municipal wastes, and other solid wastes.

Fixed bed, fluidized bed, and entrained flow gasification are the three basic types of gasification processes. Due to its adaptability and minimal environmental effect, entrained flow gasification is the commercially selected method among these processes [12]. For both economic and technical purposes, entrained flow gasifiers are especially suitable to solid fuels with low ash content, and the preferred ash content range for entrained flow bed gasifiers is 10–40 wt.% [13]. With a high throughput, the temperature of entrained bed gasification can reach 1600 °C, and the pressure can reach 3 MPa [14]. The entrained flow gasifier additionally offers better cold gas efficiency and a near 100% carbon conversion rate. They also have better thermodynamic performance, faster reaction rates, and higher reaction intensity [15]. Biomass gasification is one of several potential sustainable energy generation technologies being considered. However, the low energy density, poor storability, and geographical dispersion of biomass-based systems limit large-scale use [16]. Nonetheless, the co-gasification of biomass in large scale IGCC has already been tested [17,18]. Therefore, an IGCC adopting a biochar/waste tyre blend as fuel could be regarded as an alternative approach for increasing the volume of syngas produced, improving system efficiency, and increasing waste recovery in an effective method.

There are several efficient methods employ power sources to create electricity and other important goods. Among all of these approaches, multigeneration energy production systems have gained popularity in recent decades [19]. They are systems that produce several outputs from a single input. Alternative power generation strategies based on solid fuels, such as the IGCC, are more efficient and environmentally friendly [20]. Variety of products can be produced including hydrogen and chemicals such as methanol and higher alcohols. In addition to supplying raw chemicals, the IGCC can generate electricity with higher efficiency [1]. The performance of IGCC is determined by integration configurations and can be improved by process optimization. For example, co-production or polygeneration of steam, hydrogen and other products is an aspect to consider together with GT, air extraction to the air separator, high and low temperature heat recovery [21]. Despite the fact that there are other methodologies, this research focuses on power generating schemes based on a combined GT and Kalina cycle.

Waste heat to power is the process of capturing heat from an industrial plant and using it to generate electricity. Industrial processes produce hot exhaust gases and waste streams that can be utilized to generate power [22]. The Kalina cycle converts thermal energy from low-temperature heat sources to mechanical power. The Kalina cycle is basically a modified Rankine cycle in which the working fluid is a combination of two distinct compounds: water and ammonia [23]. Using an ammonia/water mixture provides enabling adjustable temperature properties during condensation and evaporation. For example, unlike pure component coolants, the mixture evaporates and condenses across a wide temperature range. Thus, binary mixture cycles provide a better thermal relationship between the working fluid and the heat reservoir than typical refrigerating and power cycles [24]. Many researchers suggested novel ideas [25–28] for coupling the Kalina cycle towards other thermodynamic cycles in order to achieve greater not only mechanical power but also heat and/or refrigeration while employing the Kalina cycle's high efficiency.

Energy analysis has become the standard technique for measuring the effectiveness of energy conversion processes. A system's energy inputs and outputs can be quantified with the use of an energy analysis. Energy balance, on the other hand, provides no insights into the system's degeneration through time or its irreversibilities [29]. In this context, exergy, exergy destruction, and entropy generation ideas, as well as combined evaluation methodologies, are gaining acceptance [30]. The second law of thermodynamics provides the foundation for exergy analysis, which offers a novel and informative approach to evaluate and analyze processes and systems. Exergy analysis, in particular, provides efficiencies that are more indicative of how close real performance is to the ideal, and it pinpoints the sources and locations of thermodynamic losses more precisely than energy analysis [31]. Power plants of all varieties, steam turbines, GTs, combustion engines, incinerators, cogeneration facilities, etc. are subjected to energy and exergy assessments. Both the first and second laws, as well as a comparison to other options, are considered in these analyses. Moreover, this technique could allow for a quantitative evaluation and comparison of various energy conversion technologies. The exergetic impacts can be addressed when comparing the various configurations [32].

By applying computer-aided process design, optimization, plant operation, safety operation and control, the design and simulation technique has a crucial role in the development of new technologies [33]. Instead of Aspen Plus, which can handle non-conventional solids, Aspen HYSYS was employed for the simulation in this paper. Although studies of the IGCC or Kalina cycle combined systems have been performed using diverse computational software, comprehensive research of them using the Aspen HYSYS process simulator are limited. Pierobon and Rokni [34] proposed a facility layout that included a gasification system, solid oxide fuel cell (SOFC), and a basic Kalina cycle. The fixed bed gasification system utilized woodchips as fuel, and the produced syngas was used to fuel a combined SOFC–Kalina cycle power plant. According to the authors' results, the system's thermal efficiency can range from 49% to 51% relying on the ammonia concentration. Further, by increasing the SOFC utilization factor and lowering the current density, a maximum efficiency of 58.3% can be achieved. Okeily et al. [22] developed a facility that combines a coal gasification system with a combined GT, steam turbine power plant cycles, and a Kalina cycle. Researchers evaluated key performance parameters of the Kalina cycle

and found that integrated cycle mitigates the overall efficiency loss caused by the gasifier. Recently, Ji-chao et al. [35] presented a plant that integrates a biomass gasification plant, a GT, a supercritical CO_2 cycle, and a modified Kalina cycle. Energy and exergy efficiencies were 78.15% and 40.97%, respectively, in research on the impacts of terminal difference in temperature of air preheater, compression ratio of air pump, pressure ratio of supercritical CO_2 compressor, and ammonia concentration factors on system performance. Moreover, Zoghi et al. [36] suggested a complex and novel biomass-driven multi-generation process made up of five different systems: a GT cycle, a steam Rankine cycle, an ammonia-water/LNG cycle based on a modified Kalina cycle, a thermoelectric generator, and a proton exchange membrane electrolyzer. Varieties in GT inlet temperature, compressor pressure ratio, heat recovery steam generator evaporation temperature, heat recovery steam generator, pinch temperature difference, ammonia/water vapor generator temperature, compressor inlet air mass flow rate, and ammonia mass fraction are examined in their study. The researchers reported the findings of the multigeneration system in the base scenario, which had a 59.47% exergy efficiency. Tan et al. [37] suggested a hybrid power generation system that includes biomass gasification, SOFCs, gas expanders, and the Kalina cycle. The energy efficiency for the hybrid system is 64.2% in investigations where only the fuel utilization ratio was assessed in the parametric studies. Safder et al. [38] proposed an unique multi-generation system that included a bagasse-biomass based gasifier-Brayton cycle, a Rankine cycle, a Kalina cycle, a multi-effect desalination unit, and an ejector refrigeration cycle. The suggested system was subjected to extensive energy, economic, exergy, and exergorisk assessments by the authors. According to their findings, increasing the biomass mass flow rate from 1.5 kg/s to 10 kg/s resulted in losses in total energy and exergy efficiencies of 34.42% and 50.75%, respectively, and a significant rise (43.07%) in exergy efficiency at a high compression ratio. Furthermore, a co-gasification driven power production system was developed by Yan et al. [39], and energy/exergy balance calculations were conducted using Aspen Plus. The system the authors propose consists of a gasifier, chemical looping system, SOFC, and steam turbine. Researchers examined at a few different gasifier, SOFC, and chemical looping system operating variables and found that the energy and exergy efficiency of the integrated system could be 39.9% and 37.6%, respectively. Ersöz et al. [40] developed a mechanism for producing H_2 from syngas obtained by gasification. The model presented by the authors consists of tar reforming unit, gas cleaning unit, a water–gas shift unit, and a pressure swing adsorption unit for H_2 separation. Even though the work models a gasification-driven H_2 production process carried out in Aspen HYSYS, the gasification process was not carried out in Aspen HYSYS and syngas attributes were utilized as simulation inputs. Moreover, a downdraft biomass gasification model using Aspen Plus was proposed by Tauqir et al [41]. Authors used a Gibbs energy minimization method-based modeling of the major gasification zones to analyze the impact of operational factors on LHV of syngas, cold gas efficiency, and thermal efficiency. On the other hand, the gasification system was not incorporated into a secondary cycle, and the research was conducted in the Aspen Plus, which is suitable for solid processing. Using Aspen Plus, Zang et al. [42] designed a biomass integrated gasification combined cycle for eight different plant scheme options. Gasification agents, gas turbine combustion techniques, and CO_2 capture and storage alternatives were all evaluated throughout all of the scenarios. According to the exergy analysis, the maximum exergy efficiencies are achieved by combining air gasification with an externally fired gas turbine with no CO_2 emission control (37.1%), and oxygen gasification with an externally fired gas turbine with CO_2 emission control (25.2%). Burulday et al. [43] examined the performance of producing H_2 using a syngas obtained from biomass and a renewable source based integrated power generation system. In order to assess the thermodynamic performance of the hybrid system, an exergy analysis is conducted in Aspen HYSYS. The authors reported that the incorporating the organic Rankine cycle into the process of producing H_2 was claimed to increase exergy efficiency to 55.8%. Further, in terms of energy and exergy, the solar-assisted power generation system was found to have efficiencies of 19.71% and 39.6%, respectively.

The literature review section highlights the several studies that proposed integrated models biomass-driven unit with Kalina cycle system that performing parametric assessments. To date, however, no studies have presented an integrated entrained bed gasifier/GT/Kalina cycle system using Aspen HYSYS. Due to their high carbon content, a blend of biochar and waste tyre was chosen for this research since it has never been investigated previously and is a suitable feedstock for an entrained bed gasifier. In addition, the effects of independent variables on the overall system have been reported before, but most studies have concentrated on Kalina cycle parameters. Although gasifier operating characteristics are known to affect integrated system performance, this interaction has never been studied in depth. This study also presents an in-depth analysis by conducting a thermodynamic analysis for a novel integrated system in the context of the reactions taking place, the energy being transported (both chemical and physical), and the performance of individual systems. In this investigation, the Aspen HYSYS process simulator was used instead of the more often used Aspen Plus process simulator for the examination of systems powered by solid fuels. Thus, it is aimed to fill a need in the published studies and serve as an impetus for further research. In this paper, a combined entrained bed gasifier/GT/Kalina cycle system was modeled using the Aspen HYSYS. In terms of exergy and energy yields, several case study analyses of factors that have a significant effect on critical process parameters were conducted to examine essential process efficiency improvements for individual plants and the overall system. The effects of the ER, CO_2/agent ratio, gasification temperature, ammonia/water ratio, Kalina turbine inlet pressure, Kalina turbine outlet pressure and waste tyre/fuel ratio on the combined system were investigated.

2. Methodology

2.1. Characterization of feedstock materials

The great majority of entrained bed gasifiers are large-scale and were designed for coal utilization [44]. Entrained bed gasifiers can occasionally take 10–15% biomass in a coal blend and can accept a combination of feedstocks [45]. Mono-utilization of biomass is also unsuitable due to their high moisture content, and high-ash fuels are less suited since cold gas efficiency diminishes as ash content rises [46]. Furthermore, molten biomass ash very aggressive, which causes slagging, fouling, and corrosion that significantly reducing the gasifier's lifespan. All of these criteria led to the selection of biochar and waste tyre samples with high carbon, low ash and moisture content, which are both suitable for use in the entrained bed gasifier and ecologically beneficial alternatives. Table 1 summarizes the proximate analysis and ultimate analysis data for the biochar and waste tyre used in this study.

The results of volatile matter and fixed carbon are included in the proximate analysis. Unlike Aspen Plus, Aspen HYSYS software lacks a

Table 1
Proximate analysis and ultimate analysis results of biochar and waste tyre samples.

Materials		Biochar [47]	Waste tyre [48]
Proximate analysis	Moisture	–	1.18^{ad}
	Ash	10.80^{db}	11.13^{ad}
	Volatile matter	27.70^{db}	66.18^{ad}
	Fixed carbon	61.50^{db}	21.50^{ad}
Ultimate analysis	C	80.60^{ad}	77.22^{ad}
	H	2.90^{ad}	6.72^{ad}
	N	0.50^{ad}	1.44^{ad}
	S	0.10^{ad}	1.34^{ad}
	O	1.50^{ad}	1.08^{ad}

ad: air dried basis, db: dry basis.

specialized database for heterogeneous solid fuels. In other words, Aspen HYSYS does not support specifying heterogeneous solid materials and calculating their physicochemical properties. This is another reason why developing a gasification process with Aspen HYSYS is problematic. Hence, the simulation model's feedstock stream includes the elemental analysis of the biochar and waste tyre samples together with the ash and moisture content results.

2.2. Description and modeling of the combined system

A combination of an entrained bed gasifier, a GT, and a Kalina cycle is proposed to provide a high efficiency integrated system. Aspen HYSYS was used to design and analyze all of these sections. To determine all thermodynamic characteristics for the components in the overall process, the Soave-Redlich-Kwong equation of state was chosen. Since several components are involved in each reaction, the chemical reactions in the entire process are immensely complicated. Some trace reaction products such as COS, NH_3, and SO_x were not considered in the simulation because the model used a rather basic approach to represent the reaction group. Therefore, if a sufficient entrained bed gasifier simulation can be developed, numerous case studies on the proposed model can be conducted to examine various features. Predicting the performance of energy plants is a key focus of study. As a result, a quick and precise calculation technique for syngas composition, energy and exergy efficiency of systems is extremely desirable, and further systematic researches are absolutely required. The findings of the calculations can also be used as a guide for altering operational conditions or improving technology. Nevertheless, the accuracy of the forecast varies depending on the type of gasifier. The temperature of the syngas in the entrained bed gasifier is high (generally greater than 1600 K), and the content of the discharge syngas is near to that of thermodynamic equilibrium [49,50]. This allows the entrained bed gasification process to be modelled with a single Gibbs equilibrium reactor, obviating the requirement for numerous Gibbs reactors to simulate the different zones seen in other gasifier modeling studies [51,52]. In a summary, the entrained bed gasifier model uses a single Gibbs equilibrium reactor unit block to simulate the main physical and chemical processes occurring in the gasifier, such as drying, pyrolysis, secondary reactions of volatile substances, oxidation, and gasification of feedstock material. The following are the fundamental assumptions used in this work to simplify the modeling of a integrated (entrained bed gasifier/GT/Kalina cycle) system:

- The integrated system is in a steady state, with a negligible pressure loss in the unit blocks.
- The equilibrium technique was used, which ignored the gasifier's hydrodynamic complexity.
- The ash in feedstock is inactive and has no influence on chemical processes.
- H_2, CO, CO_2, CH_4, H_2O and N_2 are the gaseous products of the entrained bed gasification process. The formation of heavy hydrocarbons and tar is not taken into account.
- All reactions occur fast and chemical equilibrium is achieved.
- The potential and kinetic energy change were neglected.
- The mixture of ammonia and water that exits the condenser is a saturated liquid.
- Isentropic efficiency (87%) governs the operation of all compressors, pumps, and turbines.
- Throttling process in valve is isenthalpic.

The flowsheet diagram of the integrated system analyzed in this research is given in Fig. 1.

The entrained bed gasifier model is comprised of one Gibbs reactor (GBR-100), one component splitter (X-103), one agent compressor (K-100), and two stream mixer unit blocks (MIX-100 and MIX-102), as illustrated in Fig. 1. The gasification agents "Air" and "CO_2" together with the fuel streams "Biochar" and "Waste tyre" are the input material streams. The "CO_2" stream includes pure CO_2, the "Air" stream has 79% nitrogen and 21% oxygen, and the "Biochar" and "Waste tyre" streams contain elemental composition, moisture, and ash data of solid

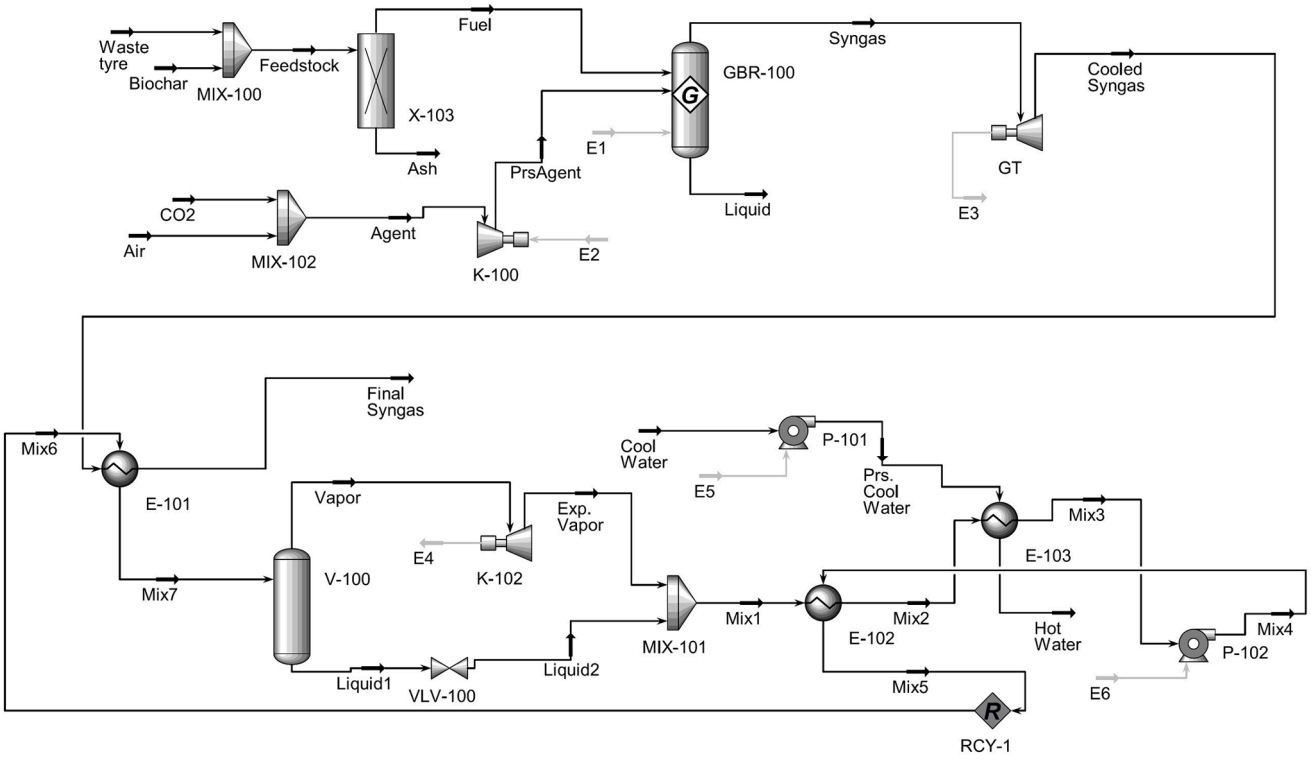

Fig. 1. Aspen HYSYS flowsheet diagram of the combined gasifier/GT/Kalina cycle process.

materials. The physicochemical properties of material streams are on as received basis. Further, the ash is separated from the "Feedstock" stream by the component splitter block "X-103″. Hence, the "Fuel" stream is on dry ash-free basis. This separation is important since the Aspen HYSYS component library lacks an inert solid element like sand. In the entrained bed gasification simulation, the synergistic activities of the ash material were also neglected, and it was considered to be absolutely inert. As a consequence, splitting the ash material prior to the reactor has no influence on the any result. The final unit block in the gasification system, the Gibbs reactor "GBR-100″, which is also the only reactor in the integrated system, conducts high-temperature activities and performs gasification reactions. The procedure thus far has only covered the entrained bed gasification phase, and it terminates with the "Syngas" stream produced at high temperature and pressure. Table 2 provides a summary of the descriptions of the system's individual building components, or unit blocks.

The high-temperature and high-pressure "Syngas" enters the GT and expands to atmospheric pressure. Thus, a large quantity of power is generated, along with "Cooled Syngas". The part of the entire system that has been viewed so far covers the entrained bed gasifier/GT plant. Afterwards, the cooled syngas is used as the thermal energy source for the Kalina cycle in this research. In the evaporator (E-101), the ammonia-water mixture is boiled, and then separated into a saturated ammonia-water vapor (Vapor) and an ammonia-water liquid (Liquid1) in the flash separator (V-100). The vapor is then passed through the turbine (K-102) to generate electricity. In the mixer unit block (MIX-101), a saturated ammonia-water liquid (Liquid1) is throttled down to a low pressure (Liquid2) and mixed with the ammonia-water vapor from the turbine. After that, the ammonia-water mixture (Mix1) is precooled in the recuperator (E-102). The ammonia-water mixture (Mix2) then cools down in the condenser (E-103) while increasing pressure via the pump (P-102). The closed system is completed when the cold ammonia/water mixture passes through the recuperator (E-102) and recycle blocks (RCY-1). Therefore, the Kalina cycle has been described, and the combined gasifier/GT/Kalina cycle system has been developed. Table 3 lists the assessed stream characteristics in the base scenario for the integrated system.

Table 2
Detailed explanations of each of the ASPEN HYSYS unit blocks.

Block ID	Aspen HYSYS UnitOPS	Function
GBR-100	Gibbs reactor	The Gibbs free energy minimization method is used to simulate reactions between reactants and determine possible products.
X-103	Component splitter	Separates the ash content in "Feedstock" stream.
V-100	Vessel	Separates the liquid and vapor phases in equilibrium at a given temperature and pressure.
MIX-100 MIX-101 MIX-102	Mixer	It combines the input streams into a single output stream.
E-101 E-102 E-103	Heat exchanger	Performs heat transfer by utilizing the energy differences of cold and hot streams.
VLV-100	Valve	Expands a high-pressure liquid to a lower pressure.
P-101 P-102	Pump	Increases pressure of the fluid in the liquid phase to higher pressures.
K-100	Compressor	Increases pressure of the fluid in the vapor phase to higher pressures.
GT K-102	Expander (Turbine)	Decreases pressure of the fluid in the vapor phase to lower pressures.
RCY-1	Recycle	Links "Mix5" and "Mix6" streams to provide recycling.

Table 3
Stream properties in the base scenario for the combined entrained bed gasifier/GT/Kalina cycle plant.

Material Streams	Vapor fraction	Temperature (°C)	Pressure (bar)	Flow rate (kg/h)
Waste tyre	0.33	25.00	20.00	200.00
Biochar	0.17	25.00	20.00	800.00
Feedstock	0.21	25.00	20.00	1000.00
Fuel	0.22	25.00	20.00	891.30
Ash	0.00	25.00	20.00	108.70
CO_2	1.00	20.00	1.01	603.10
Air	1.00	20.00	1.01	3558.00
Agent	1.00	19.96	1.01	4161.00
PrsAgent	1.00	424.80	20.00	4161.00
Syngas	1.00	1500.00	20.00	5052.00
Liquid	0.00	1500.00	20.00	0.00
Cooled Syngas	1.00	700.00	1.00	5052.00
Final Syngas	1.00	175.20	1.00	5052.00
Mix1	0.60	110.40	8.00	3009.00
Mix2	0.49	92.42	8.00	3009.00
Mix3	0.00	25.10	8.00	3009.00
Mix4	0.00	25.43	30.00	3009.00
Mix5	0.00	82.16	30.00	3009.00
Mix6	0.00	82.16	30.00	3009.00
Mix7	0.58	160.00	30.00	3009.00
Vapor	1.00	160.00	30.00	1716.00
Liquid1	0.00	160.00	30.00	1293.00
Exp.Vapor	0.94	107.20	8.00	1716.00
Liquid2	0.15	116.20	8.00	1293.00
Cool Water	0.00	25.00	1.01	11000.00
Prs.Cool Water	0.00	25.03	6.00	11000.00
Hot Water	0.00	84.44	6.00	11000.00

2.3. Gibbs free energy minimization

Chemical equilibrium analysis can be used to determine the maximum per-pass conversion that can be achieved as well as the composition of the reaction mixture at equilibrium. As a result, it could identify ways to improve both conversion and selectivity [53]. The Gibbs free energy is a thermodynamic potential that estimates the usable or process-initiating work that an isothermal, isobaric thermodynamic process may produce. The chemical potential that is lowest when a system reaches equilibrium at constant pressure and temperature is known as Gibbs energy [54]. In stoichiometric modeling, which equilibrium constants for individual reactions in the process is determined, all of the reactions that take place throughout the gasification process must have stoichiometric coefficients, and the equilibrium constants should be determined accordingly. On the other hand, without defining the stoichiometry, Gibbs free energy minimization provides an attractive methodology. The Gibbs reactor unit block (GBR-100), which employs Gibbs free energy minimization method to compute the chemical equilibrium of a list of substances, is used to determine gasification products. The system's Gibbs free energy is minimized when the gasification activities reach equilibrium:

$$G^t = \sum_{i=1}^{N} n_i \mu_i \tag{1}$$

where n_i and μ_i denote the number of moles and chemical potential of species i respectively.

$$\mu_i = G_i^m + RTln(f_i/f_i^m) \tag{2}$$

where G_i^m stands for the universal standard Gibbs free energy, whose value is unaffected by the kind of gas and is simply related to the unit. R is the universal gas constant, T is the temperature, and f_i and f_i^m are the fugacity and standard fugacity of species i respectively. At standard pressure, μ_i can be stated as follows:

$$\mu_i = \Delta G_{f,i}^m + RTln(x_i) \tag{3}$$

where x_i stands for the molar fraction of gas species i and $\Delta G_{f,i}^m$ stands

for the standard Gibbs free energy for the formation of species *i*. The Lagrange multiplier approach is used to compute the value of n_i for which the total Gibbs free energy of the system is minimized by substituting (Eq.3) into (Eq.1).

$$(\partial L/\partial n_i) = \Delta G^m_{f,i} + n_i RTln(n_i/n_{total}) + \sum_{j=1}^{k} \lambda_j a_{ij} = 0 \quad (4)$$

where the number of atoms of the j_{th} element in a mole of the i_{th} species is a_{ij}, and the Lagrange function and multiplier are L and λ_j, respectively. Eq. (4) is used to generate a set of iteratively solveable nonlinear equations.

2.4. Energy and exergy analysis

Two of the most important criteria to consider when analyzing and defining system performance are thermal energy and exergy. The exergy analysis approach examines the energy quality and usability of a system by estimating its effectiveness. The exergy assesses the system's transition from an environment state to a dead state, including any potential change streams. Physical exergy, chemical exergy, potential exergy, and kinetic exergy are all included in total exergy. On the other hand, the potential exergy and kinetic exergy are generally ignored in thermodynamic systems like gasifiers since they are associated with velocity and elevation, which have minimal variations throughout the gasification process [55]. Generally, the summation of the physical and chemical exergies in a stream of substance can be used to quantify the available exergy. In addition, the lower heating value (LHV) is commonly used to determine the quantity of usable fuel energy available. As a result, determining the syngas LHV and exergy achieved at the conclusion of the gasification process is critical. The LHV and physical exergy values of syngas can be acquired from the stream properties section of the Aspen HYSYS simulator, but the chemical exergy value must be calculated externally. In practice, the values were extracted from the process simulator's property results for the streams and unit blocks and converted to the "kW" unit. The energy (Eq.5) and physical exergy (Eq.6) [56] of material streams are calculated as follows:

$$\dot{e}_{stream} = \dot{m}(h_2 - h_1) \quad (5)$$

$$\varepsilon_{ph} = \Delta h - T_0 \Delta s = (h - h_0) - T_0(s - s_0) \quad (6)$$

For the chemical exergy calculation, the exergy of all the components of a system must be determined before the analysis. To accomplish so, a state of the environment was defined, which included temperature, pressure, and the chemical components of the environment. The chemical exergy equation for a mixed gas, such as syngas, with several components is as follows [55]:

$$EX_{ch} = \sum y_i EX^0_{ch} + RT_0 \sum y_i \ln(y_i) \quad (7)$$

where R is the universal gas constant, T_0 is the ambient (reference) temperature (298.15 K), y_i is a gaseous component's molar fraction, and EX^0_{ch} is a gaseous component's standard chemical exergy [57]. Solid fuels, such as biomass and char, are, on the other hand, unconventional compounds whose exergy is difficult to calculate. A method of determining chemical exergy for solid fuels was employed in this simulation procedure. Since the feedstock material is supplied to the gasifier at ambient temperature, the physical exergy of the feedstock material is minimal, and only the chemical exergy is considered. The chemical exergy of solid fuel is computed as follows [58]:

$$\varepsilon_{ch,solidfuel} = ß^* LHV_{solidfuel} \quad (8)$$

Szargut and Styrylska [59] derived "β" using statistical correlations for solid biofuels, where "β" is a coefficient that given the ratio of chemical exergy to LHV:

$$ß = \frac{1.0414 + 0.0177\frac{H}{C} - 0.3328\frac{O}{C}\left\langle 1 + 0.0537\frac{H}{C}\right\rangle}{1 - 0.4021\frac{O}{C}} \quad (9)$$

where C, H and O are the atomic ratios. Carbon conversion efficiency, cold gas efficiency, thermal efficiency, CO_2, SO_2 and NO_x emission volumes per unit of net power generation, and other performance metrics can be evaluated in thermodynamic, economic, or environmental perspectives. Thermal efficiency, on the other hand, is frequently preferred as a measure of total process efficiency. This is a measure of the total efficiency of the process. The overall thermal efficiency of the integrated system is expressed as follows:

$$\eta_{energy,overall} = \frac{(P_{produced} - P_{auxiliary}) + \dot{E}_{finalsyngas}}{\dot{E}_{feedstock}} \times 100 \quad (10)$$

where $\dot{E}_{finalsyngas}$ ($LHV_{\text{finalsyngas}} \times \dot{m}_{finalsyngas}$) is the total calorific value of final syngas and $\dot{E}_{feedstock}$ ($LHV_{\text{feedstock}} \times \dot{m}_{feedstock}$) is the total calorific value of feedstock material entering the Gibbs reactor. The generated power from the turbines is $P_{produced}$ and auxiliary power consumption in pumps, compressors, etc. is $P_{auxiliary}$. For entrained bed gasifier thermal efficiency:

$$\eta_{energy,gasifier} = \frac{(P_{consumed} + \dot{E}_{syngas})}{\dot{E}_{feedstock}} \times 100 \quad (11)$$

where $\dot{E}_{syngas}$ ($LHV_{syngas} \times \dot{m}_{syngas}$) and $\dot{E}_{feedstock}$ ($LHV_{\text{feedstock}} \times \dot{m}_{feedstock}$) are the total calorific value of syngas and feedstock material, respectively. Since the gasification process is endothermic and requires power to increase the gasifying agent to high pressures, the term power is subscripted as consumed. A similar thermal efficiency formulation for the gasifier/GT system is expressed as:

$$\eta_{energy,gasifier/gasturbine} = \frac{(P_{consumed} + P_{gasturbine} + \dot{E}_{cooledsyngas})}{\dot{E}_{feedstock}} \times 100 \quad (12)$$

where $\dot{E}_{cooled\ syngas}$ ($LHV_{cooled\ syngas} \times \dot{m}_{cooled\ syngas}$) and $\dot{E}_{feedstock}$ ($LHV_{\text{feedstock}} \times \dot{m}_{feedstock}$) are the total calorific value of cooled syngas and feedstock material, respectively, $P_{consumed}$ denote the power required for the entrained bed gasification system. The power obtained from the GT is added to the numerator in addition to the gasifier system thermal efficiency formulation. Lastly, the Kalina cycle's energetic efficiency is calculated as follows:

$$\eta_{energy,Kalina} = \frac{P_{Kalina} - P_{auxiliary}}{\dot{m}_{cooledsyngas/finalsyngas}(h_{cooledsyngas} - h_{finalsyngas})} \times 100 \quad (13)$$

where P_{Kalina} indicates the power obtained from the Kalina turbine, $P_{auxiliary}$ indicates the power consumed by the pumps, the mass flow rates for the cooled syngas or final syngas streams are represented as $\dot{m}_{cooled\ syngas/final\ syngas}$, and the specific mass enthalpy values for the associated streams are denoted as $h_{cooled\ syngas}$ and $h_{final\ syngas}$.

The efficiency of exergy is regarded as second-law efficiency, and it is commonly defined as consumed exergy divided by supplied exergy. The terms consumed exergy and supplied exergy have a variety of interpretations. The overall exergy efficiency of the integrated system is described as follows:

$$\eta_{exergy,overall} = \frac{(P_{produced} - P_{auxiliary}) + \varepsilon_{ch,finalsyngas} + \varepsilon_{phy,finalsyngas}}{\varepsilon_{ch,feedstock} + \varepsilon_{phy,agent}} \times 100 \quad (14)$$

where $\varepsilon_{ch,finalsyngas}$ and $\varepsilon_{phy,finalsyngas}$ are the chemical exergy and physical exergy values for the final syngas stream. The generated power from the turbines is $P_{produced}$ and auxiliary power consumption in pumps, compressors, etc. is $P_{auxiliary}$. Furthermore, a gasifier model's exergetic efficiency can be described as follows:

$$\eta_{exergy,gasifier} = \frac{P_{consumed} + \varepsilon_{ch,syngas} + \varepsilon_{phy,syngas}}{\varepsilon_{ch,feedstock} + \varepsilon_{phy,agent}} \times 100 \quad (15)$$

where $\varepsilon_{ch,syngas}$ and $\varepsilon_{phy,syngas}$ denote the chemical exergy and physical exergy of syngas respectively, $\varepsilon_{ch,feedstock}$ the chemical exergy of feedstock material, and $\varepsilon_{phy,agent}$ the physical exergy of gasification agent. A similar exergetic efficiency formulation for the gasifier/GT system can

be written as follows:

$$\eta_{exergy,gasifier/gasturbine} = \frac{(P_{consumed} + P_{gasturbine} + \varepsilon_{ch,cooledsyngas} + \varepsilon_{phy,cooledsyngas})}{\varepsilon_{ch,feedstock} + \varepsilon_{phy,agent}} \times 100 \quad (16)$$

where $\varepsilon_{ch,cooledsyngas}$ and $\varepsilon_{phy,cooledsyngas}$ denote the chemical exergy and physical exergy of cooled syngas respectively, $\varepsilon_{ch,feedstock}$ the chemical exergy of feedstock material, and $\varepsilon_{phy,agent}$ the physical exergy of gasification agent. Similar to the energetic efficiency formulation, the power obtained from the GT is added to the power consumed by the entrained bed gasification system. Finally, the Kalina cycle's exergetic efficiency is calculated as follows:

$$\eta_{exergy,Kalina} = \frac{P_{Kalina} - P_{auxiliary}}{\dot{m}_{cooledsyngas/finalsyngas}(s_{cooledsyngas} - s_{finalsyngas})} \times 100 \quad (17)$$

where P_{Kalina} indicates the power obtained from the Kalina turbine, $P_{auxiliary}$ indicates the power consumed by the pumps, the mass flow rates for the cooled syngas or final syngas streams are represented as $\dot{m}_{cooled\ syngas/final\ syngas}$, and the specific mass exergy values for the related streams are denoted as $s_{cooled\ syngas}$ and $s_{final\ syngas}$.

3. Results

3.1. Model validation

The composition of the syngas was compared with the results of experimental studies in the literature to determine the reliability of the newly proposed entrained bed gasifier model. In the experimental research, the gasification process was simulated considering input factors such as gasification temperature, feedstock material properties, solid fuel and gasifier flow rates, etc. The experimental results for three types of feedstock materials are compared with the syngas composition predicted by the entrained flow gasifier model, as depicted in Fig. 2.

It is critical to verify the simulation model before proceeding with parametric work on the entrained bed gasifier model. Because an inaccurate model cannot be trusted, and correct conclusions cannot be made. Since the fuels employed in this investigation are biochar and waste tyre samples, validation procedures were performed on three specific types of solid fuels. As examined in Section 2.1, the H/C and O/C ratios for the biochar sample are 0.432 and 0.014, respectively, while the H/C and O/C ratios for the waste tyre sample are 1.044 and 0.010, respectively. These two feedstock materials have a higher degree of carbonization than biomass or peat, hence it can be stated that they are in the coal class, according to the Van Krevelen diagram [63]. Therefore, the newly proposed entrained bed gasification model has been verified utilizing biomass, lignite, and subbituminous gasification processes. The "experimental" columns show the results of experimental research that has been published in the literature. In addition, the "model" columns show the findings of the entrained bed gasifier model developed in this study. Validation results demonstrate that the difference between the model prediction and experimental data is acceptable, indicating that the model can be applied to forecast gasification product attributes. We were able to acquire findings that were consistent with the experimental results because the entrained bed gasifiers are run at high temperatures, the conversion occurs fast, and the reactions reach chemical equilibrium. As a consequence, the entrained bed gasifier simulation can model the gasification process and produce consistent results during parametric studies.

An entrained bed gasifier and a Kalina cycle are used in the integrated system under study. As a result, a validation of the proposed Kalina cycle model is also crucial. Table 4 summarizes the comparison of data from the literature [64] with expected outcomes from the proposed Kalina cycle model. The estimated values are observed to be compatible with the literature.

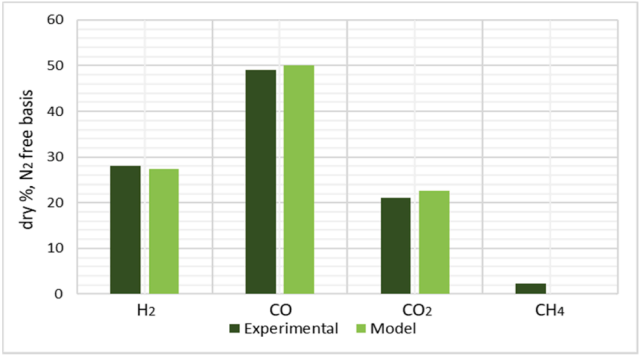

(a)

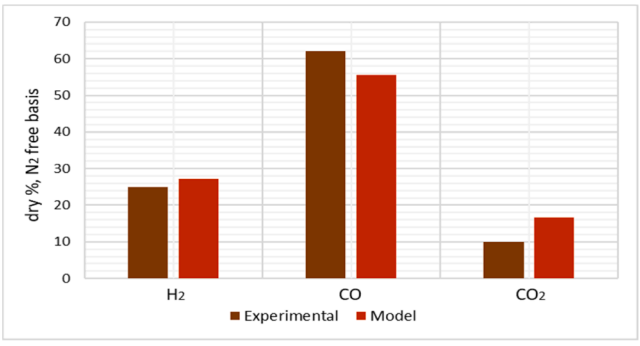

(b)

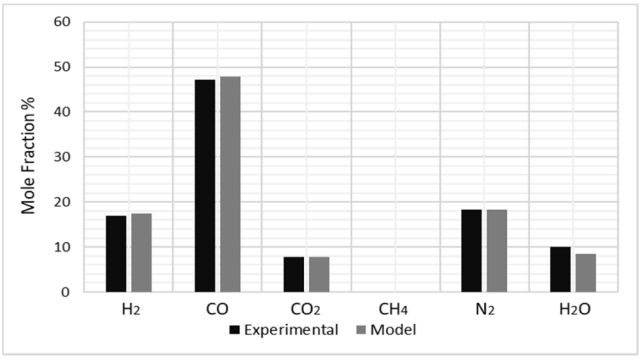

(c)

Fig. 2. A comparison of the syngas compositions obtained from experiments with those acquired by modeling an entrained bed gasifier (a) Stem wood powder [60] (b) Indonesian Baiduri (subbituminous) coal [61] (c) Inner-Mongolia lignite [62].

3.2. Parametric study

The influence of independent variables was observed and those associated variables, i.e. the dependent variables, were adjusted using seven sensitivity analyses (case study module). Gasification temperature, ER, CO_2 ratio in gasifying agent, tyre/feedstock ratio, ammonia/water ratio, and pressure before and after Kalina turbine were chosen as variables with a high impact on the outcomes. Within each case study, the main parameters in terms of thermal and exergetic efficiency on the gasifier, gasifier/GT, Kalina cycle, and overall system were evaluated. While performing a parametric research on one of the independent variables, the other independent variables are maintained constant at the base scenario value. Table 5 lists the range of independent operating variables for the parametric study, as well as the values of each variable in the base case.

3.2.1. Effect of ER

The ER is the proportion of oxygen in the gasifying agent to the

Table 4
A comparison of the results obtained by using a Kalina cycle driven by hot water.

Stream ID	Temperature (°C)		Pressure (MPa)		Ammonia Fraction (%)		Mass Flow (kg/s)	
	This study	**Literature** [64]	**This study**	**Literature** [64]	**This study**	**Literature** [64]	**This study**	**Literature** [64]
Mix7	91.00	91.0	2.7	2.7	0.800	0.80	2.966	2.97
Vapor	91.00	91.0	2.7	2.7	0.989	0.99	1.534	1.52
Liquid1	91.00	91.0	2.7	2.7	0.596	0.60	1.431	1.45
Exp.Vapor	30.59	30.7	0.79	0.79	0.989	0.99	1.534	1.52
Liquid2	49.19	49.9	0.79	0.79	0.596	0.60	1.431	1.45
Mix1	46.38	46.8	0.79	0.79	0.800	0.80	2.966	2.97
Mix2	25.00	25.0	0.79	0.79	0.800	0.80	2.966	2.97

Table 5
Independent operational variables for the purpose of the parametric research.

Parameter	Range	Base Scenario Value
ER	0.2 – 0.4	0.3
Tyre/fuel ratio (wt./wt.)	0.1 – 0.9	0.2
Gasifier temperature (°C)	1300–1700	1500
CO_2/agent ratio (vol./vol %)	2.5–10	10
Ammonia/water ratio (vol./vol %)	40–80	60
Pressure before the Kalina turbine (bar)	20–40	30
Pressure after the Kalina turbine (bar)	7–16	8

amount needed for complete stoichiometric combustion [65]. It is a significant determinant of syngas quality. Therefore, the composition of the syngas highly changes depending on the ER. Fig. 3 demonstrates the change of syngas content depending on the ER.

As the amount of air in the gasifier grows, so does the concentration of oxygen of the reactant, resulting in a boosting of the oxidation reaction and a reduction in CO concentration in syngas. The CO content reduced from 44% to 30% when the ER increased from 0.2 to 0.4. Other gaseous components, on the other hand, did not have a constant profile that changes with the ER. For the entrained bed gasification process, ER = 0.29 seems to be a specific point. At this ER, the CO content in the syngas has dropped dramatically, while the N_2 concentration has started to rise sharply. Beyond this ER value, it is reasonable to assume that complete combustion prevails over partial oxidation (gasification). Further, the N_2 content raised as a result of supplying excessive amount of air to the gasifier. Also, the concentrations of H_2O and CO_2 increased as a result of the combustion reactions. Beyond ER = 0.29, there is no CH_4 concentration, and ER = 0.25 seems to be optimal for maximizing CH_4 concentration. At ER = 0.25, the CH_4 concentration reaches 5.6%, but at ER = 0.3, it is totally depleted. The shift in CH_4 concentration can be explained by the equilibrium states of methane formation and methane reforming processes. Moreover, at ER = 0.29, the H_2 concentration reached a peak of 9.6%. Beyond this ER, the dominance of combustion reactions may also be inferred from the trend of rising H_2O concentration with decreasing H_2 concentration. Additionally, the reason why CO is the gas component with the highest concentration after N_2 can be explained by the increase in the amount of CO_2 fed with the increasing ER (10% CO_2 of the gasifying agent) and the forward shift of the Boudouard reaction. This variation in syngas composition correlates with the stated 0.2–0.4 ER interval for efficient gasification in the literature [66]. The syngas composition is considerably changed by the ER, as can be observed from the concentration profiles of the gaseous - components, and consequently the energetic and exergetic efficiency profiles alter. Fig. 4 depicts the variance in energetic and exergetic efficiency for individual and overall systems as a function of ER change.

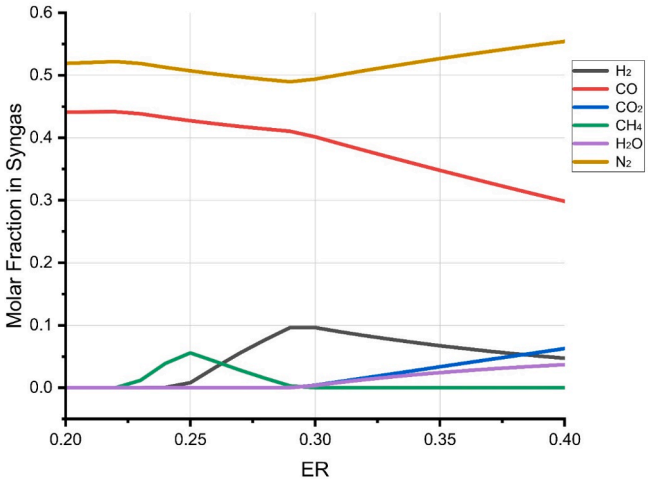

Fig. 3. Variation in gaseous component concentrations in syngas depending on the ER.

With the exception of the Kalina cycle, energetic and exergetic efficiency increased at first, peaked, and subsequently declined. Furthermore, the optimum ER values, where both energy and exergy efficiencies are maximized, fall within the required range of 0.2 to 0.4. The gasifier with the highest energy efficiency (71.85%) has an ER of 0.24. Although the concentration of H_2 peaks at ER = 0.29, the concentration of CO steadily reduces as ER rises, while the concentration of components such as N_2 and H_2O, which reduce syngas' calorific value, increases. Furthermore, at ER = 0.25, the CH_4 concentration reaches its maximum (5.6%), contributing approximately 3 times more to the syngas LHV than H_2 and CO [67]. Increasing the ER over roughly 0.25 resulted in a decrease in efficiency due to a parallel reduction in the concentration of favorable gas components, since the energy efficiency of gasification is directly related to the concentration of combustible gas components. The gasifier's exergetic efficiency increases remarkably between 0.20 and 0.25 (from 49.23% to 84.51%) and then decreases by around 2% before almost stabilizing at 82.50%. Exergy efficiency, in contrast to energy efficiency, is influenced by the syngas temperature and the concentration of non-combustible gases. As anticipated, higher ER favors exothermic reactions, resulting in a decrease in energy provided to the gasifier. However, the amount of energy needed to bring the gasifying medium to the gasification temperature rises linearly with the quantity of air delivered to the reactor. Increasing the agent feed rate to the gasifier continuously also increases the workload on the compressor. Thus, the energy and exergy efficiency is influenced by the combined impacts of the syngas composition and the quantity of power required for the equipment. To conclude, considering the energetic and exergetic efficiency for the gasifier, the optimal ER range seems to be between 0.20 and 0.25. When comparing the energetic and exergetic efficiency of the gasifier/GT system to that of the gasifier system, it is noticeable that they are quite similar. However, whereas exergetic efficiency declines by 0.6% for the same ER values, energy efficiency increases considerably. The gasifier/GT system has an energy efficiency of 85.48% at ER = 0.23. This result is 13% greater than the gasifier system's maximum energy efficiency. This can be explained by the fact that using the GT generates more power without affecting the composition of the syngas produced. The physical exergy of the cooled syngas decreases, which indicates the reduction in exergetic efficiency. In addition, ER shifts do not appear to have a major impact on the Kalina cycle. Energy efficiency

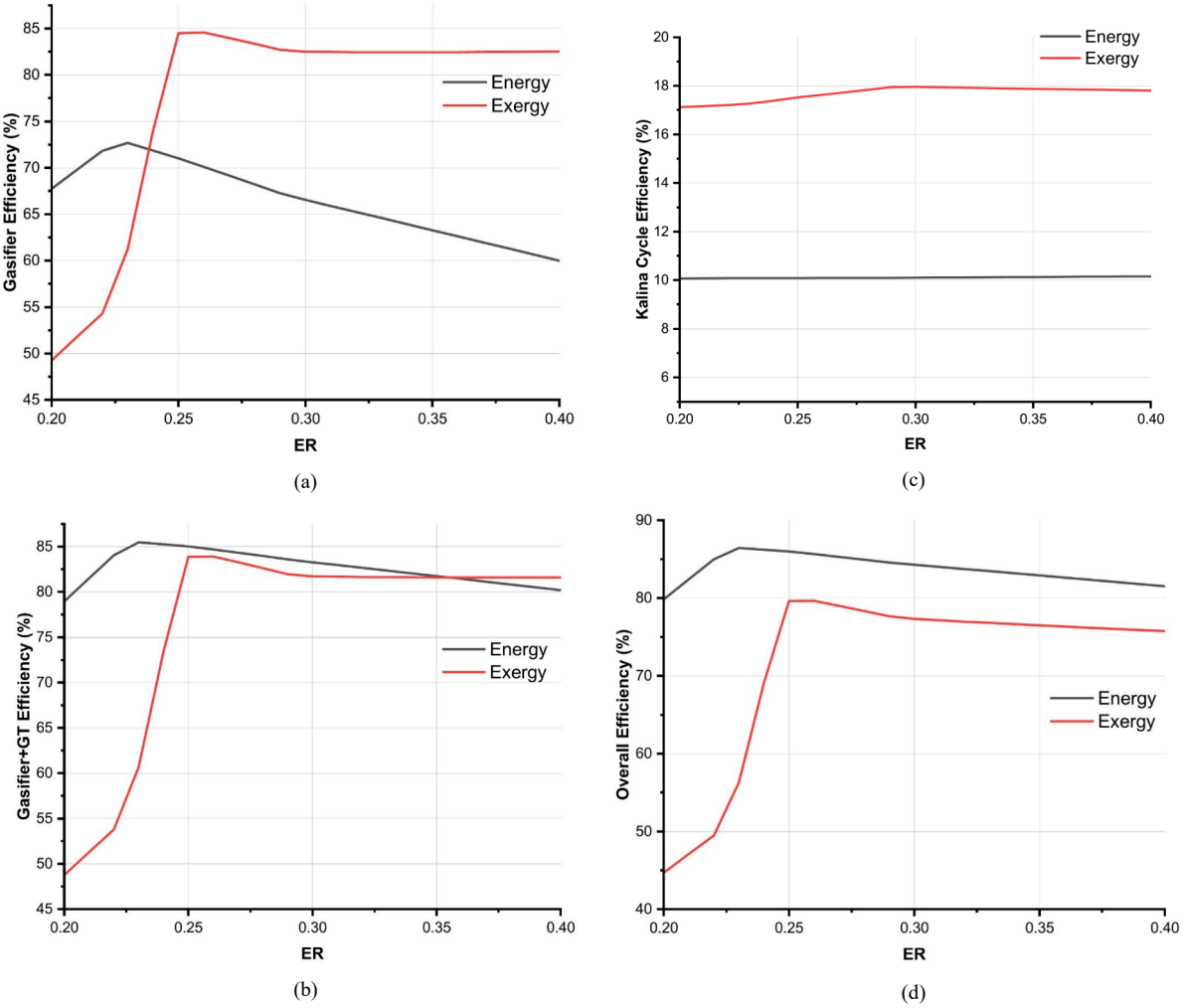

Fig. 4. Impact of ER on the energy and exergetic efficiencies of individual systems and the overall plant.

improves by 0.1% while ER increases between 0.2 and 0.4. At ER = 0.3, exergetic efficiency reaches its peak (17.96%) for the Kalina cycle. Lastly, the overall system's energy and exergy efficiency profiles are quite identical to the gasifier/GT system's. Integrating the Kalina cycle with the gasifier/GT system, on the other hand, increased the overall system's energy efficiency by around 1%. Singh and Kaushik [68] modelled a Kalina cycle integrated with a coal-fired steam power plant, and implementation of Kalina cycle increased the overall energy efficiency by 0.277% and exergy efficiency by 0.255%. Moreover, there was a 5% decrease in exergetic efficiency. The reason for this is that towards the ending of the overall system, the syngas, whose thermal energy is used in the Kalina cycle, has a lower temperature.

3.2.2. *Effect of tyre/fuel ratio*

The waste tyre/fuel ratio refers to the waste tyre's weight fractions in the feedstock. The feedstock characteristic and thermochemical process will be affected by changes in the proportion of biochar and waste tyre in the blending. Fig. 5 illustrates the change of syngas composition depending on the tyre/fuel ratio. H_2 and H_2O concentrations increase as the waste tyre/fuel ratio rises from 0.1 to 0.9, while CO and N_2 concentrations decrease. Because waste tyres have a greater H content than biochar, they produce more H_2 and H_2O [69]. The H_2 fraction increases from 9% to 13.5%, whereas the CO fraction decreases from 40% to 35.9%.

Furthermore, CO_2 and H_2O concentrations increased from quite low concentrations to roughly 1.5%. Nevertheless, it cannot be stated that

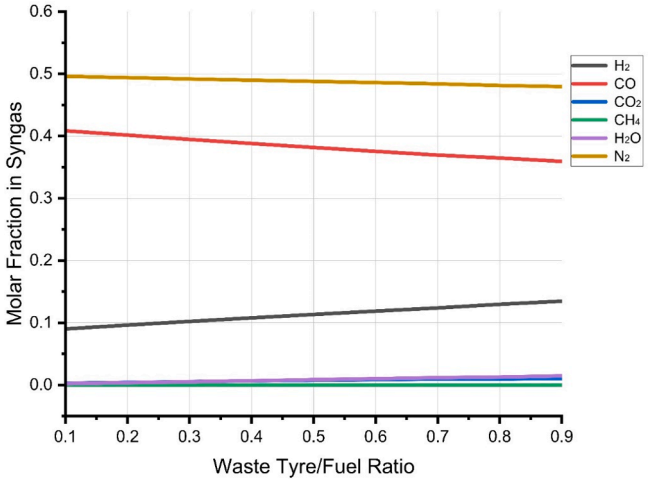

Fig. 5. Variation in gaseous component concentrations in syngas depending on the waste tyre/fuel ratio.

the feedstock characteristic causes considerable changes in syngas composition. This might be because of the similarities in composition between the two feedstock materials. The proportions of volatile matter and fixed carbon in biochar and waste tyre are quite different. However, with Aspen HYSYS, only ash and moisture from the proximate analysis

are used into the computation, unlike Aspen Plus's comprehensive list of variables. Ash and moisture content comparisons between the two solid fuels reveal their similarities. Also, both solid fuels have considerably high carbon content and low oxygen content. To conclude, it can be stated that the aforementioned distinction between the two fuels—the hydrogen content—is might be the only reason of the observed variances in syngas composition. Fig. 6 demonstrates the variance in energetic and exergetic efficiency for individual and overall systems as a function of waste tyre/fuel ratio.

The concentration of waste tyres in fuel has a minor influence on total efficiency (~0.4%), as given in Fig. 6. The greater energy efficiency could be attributed to the production of a syngas with a high calorific value due to lower N_2 concentrations (from 49.6% to 47.9%) and a higher H_2 concentration. The Kalina cycle, contrarily, appears to be unaffected by the feedstock's physicochemical properties. Energy efficiency remained at 10.10%, while exergy efficiency remained at 17.96%. Additionally, both the entrained bed gasifier and the gasifier/GT system show similar trends. The exergetic efficiency of both systems declines when the waste tyre ratio in the feedstock grows, whereas the energetic efficiency improves. The gasifier's energy efficiency improves from 66.50% to 66.83%, while its exergy efficiency drops from 82.55% to 82.26%. While the energy efficiency of the gasifier/GT system increases from 82.23% to 83.60%, the exergy efficiency decreases from 81.77% to 81.48%. Unlike other operational parameters, the syngas composition does not vary considerably, and this is correlated with the absence of substantial changes in energy efficiency and exergy efficiency. Although CO is an important substance for the thermal quality of syngas, energy efficiency may have improved due to a combination of factors, including a decrease in H_2O and an increase in H_2 concentrations.

3.2.3. *Effect of gasification temperature*

The gasification process involves a significant number of complicated, homogeneous, and heterogeneous reactions since it corresponds to the thermal decomposition (partial oxidation) of solid fuels. As a result, the temperature of the gasifier influences the direction of several endothermic and exothermic reactions in the reactor, resulting in changes in the concentrations of the components to be produced. Fig. 7 shows the change of syngas composition depending on the gasification temperature.

The fraction of gas components alters slightly when the gasifier temperature is changed between 1300 and 1700 °C, as depicted in Fig. 7. The H_2 concentration of 9.6%, the CO concentration of 40.1%, and the N_2 concentration of 49.4% are the most notable components. Other gases are in trace amounts. This can be attributed that the conversion has already been achieved at high temperatures and the thermodynamic equilibrium has been achieved. Also, the forward shift of the Boudouard reaction due to the gasifying agent's higher CO_2 content compared to standard air could be the explanation for the high concentration of CO. Moreover, since the entrained bed gasifier is operated at high temperatures, the Boudouard reaction, which is an endothermic reaction, is shifted forward. For the gasification process in the entrained bed reactor, other researchers have also noticed that CO predominates in the syngas composition [70]. In addition, a slight variation of syngas

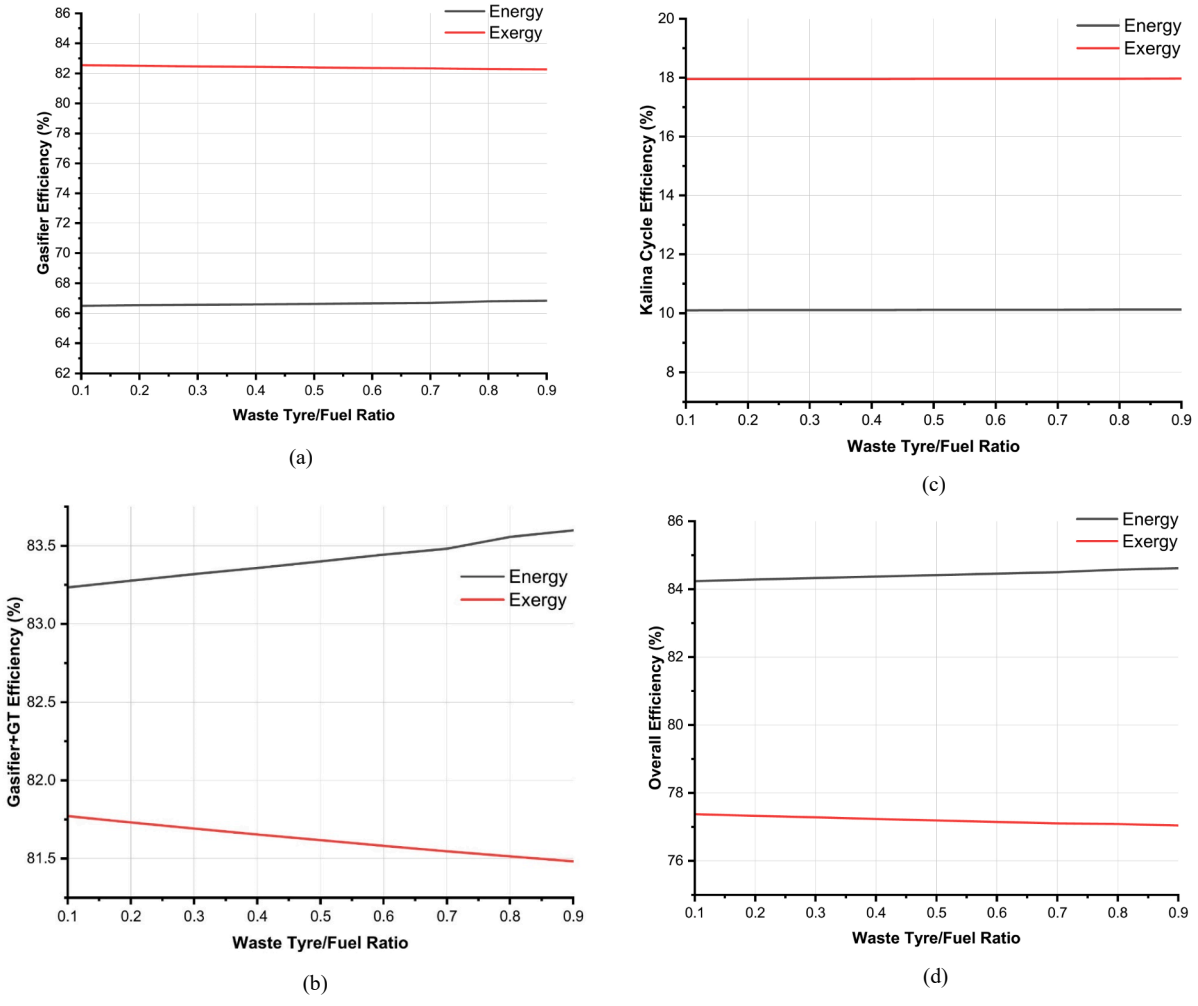

Fig. 6. The effect of the waste tyre/fuel ratio on the energetic and exergetic efficiencies of individual systems and the overall system.

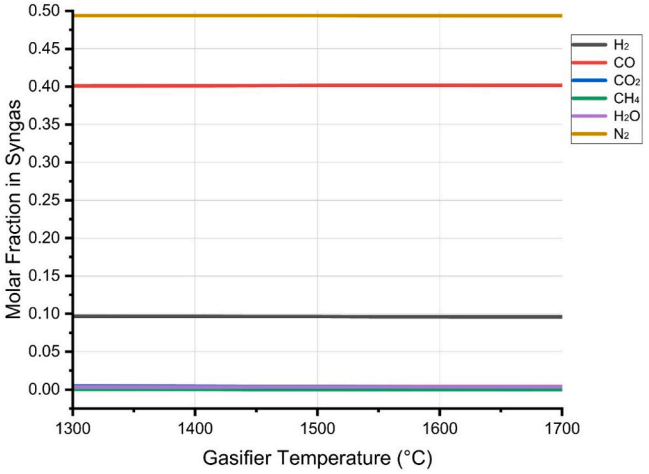

Fig. 7. Variation in gaseous component concentrations in syngas depending on the gasification temperature.

composition during high temperature gasification processes in an entrained bed gasifier has also been reported by other researchers [70,71]. Although the syngas composition is critically unaffected by the variation in high operational temperatures of the entrained bed gasifier, it has an influence on the efficiency of individual and overall systems owing to factors such as supplying the required energy and synthesizing the gas at high temperatures. Fig. 8 illustrates the variance in energetic and exergetic efficiency for individual and overall systems as a function of gasification temperature.

For all individual and overall systems, it has been observed that lower gasification temperatures perform better in terms of energy efficiency and exergetic efficiency. The overall efficiency decreased from 86.59% to 81.93% when the gasifier operating temperature was increased from 1300 °C to 1700 °C. Further, the exergetic efficiency decreased from 79.06% to 76.06% within the identical gasifier temperature change. The energy efficiency of the gasifier system has reduced from 70.81% to 62.25%, and the exergy efficiency has decreased from 83.24% to 81.86%. The increase in energy supplied to achieve higher reactor temperature may possibly explain the loss in energy efficiency. The composition of syngas does not change significantly, but the amount of energy that must be provided does. Similar conclusions can be drawn for the loss in exergy efficiency, but the physical exergy obtained is high since the temperature of the syngas produced at high gasifier temperatures increases. Chemical exergy does not alter significantly. Therefore, the decrease in exergy efficiency is not as severe as the reduction in energy efficiency. Decreased efficiency under high temperature conditions for the entrained bed gasification process was also reported by Tremel et al. [16]. The authors state that a shift of 100 °C in the gasification temperature can influence the efficiency of the process by up to 2.5%. Based on our modeling findings, it is found that a temperature rise of 400 °C reduced efficiency by around 8%. This confirms that the outcome of our simulation is consistent with the literature. The gasifier/GT system has a lower energy and exergy reduction than the gasifier system. Exergetic efficiency decreased from 82.46% to 81.08%, while energetic efficiency decreased from 85.59% to 80.93%. The total energy provided to the reactor for high-temperature operations affects energy efficiency, but an integrated GT generates power through using hot syngas' energy. The gasifier temperature change between 1300 and 1700 °C had no influence on the energy efficiency (10.10%) of the Kalina cycle, although the final syngas was achieved at a higher temperature. Exergy efficiency, on the other hand, dropped from 21.90% to 15.95%. The Kalina turbine generated greater power as the gasifier temperature increased, but the specific exergy value between cooled syngas and final syngas also increased. As a consequence, the higher gasifier temperature lowered exergetic

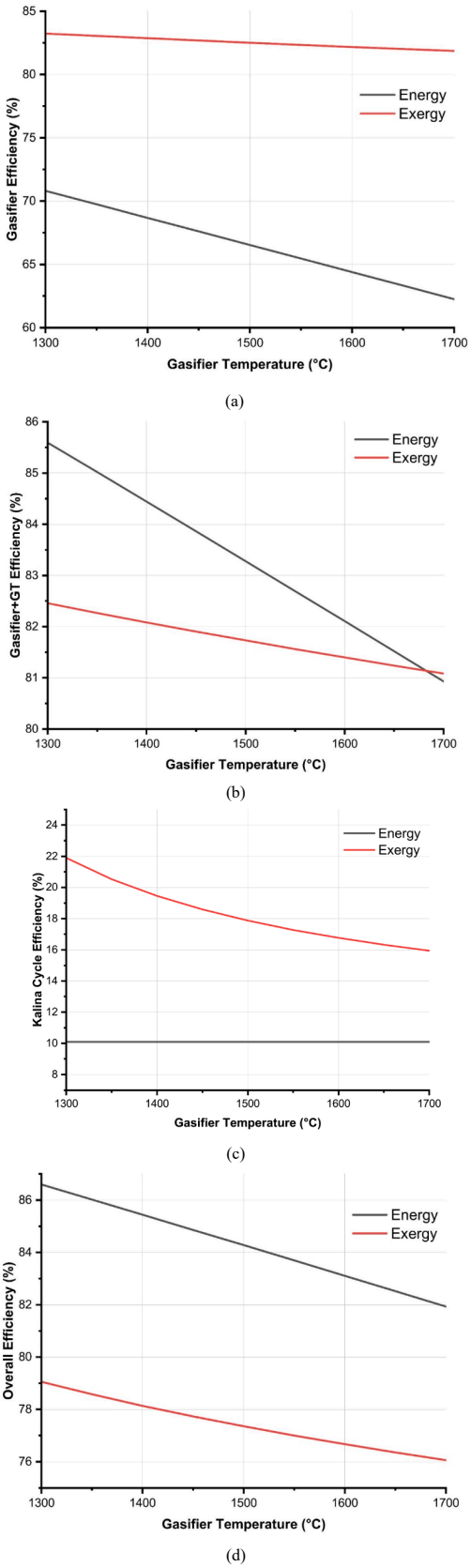

Fig. 8. The effect of gasifier temperature on the energetic and exergetic efficiencies for individual systems and the overall system.

efficiency.

3.2.4. Effect of CO_2/agent ratio

The selection of gasification agent has a substantial impact on syngas composition, and hence on individual and overall energy and exergy efficiency. Although it is convenient and inexpensive to use air as a gasification agent, the nitrogen percentage of the syngas is considerable. In addition, CO_2 gasification has lately gained interest for its particular benefits since it reacts with char at high temperatures through the Boudouard reaction or with tar by dry reforming to provide CO-enriched gas for possible applications [72]. CO_2 gasification, on the other hand, depends on highly endothermic activities such as the Boudouard reaction, and an elevated CO_2 input concentration may cause the system to fail in real-world operations. Hence, it is critical to investigate the CO_2 content in the gasification agent since it has an impact on the quality of the syngas produced, as well as the overall system efficiency. Fig. 9 depicts the change of syngas composition depending on the CO_2/agent ratio (vol.%).

H_2 and CO concentrations increase when CO_2 concentrations increase in the gasifier, whereas N_2 and CH_4 concentrations reduce. The decrease in N_2 concentration may be attributed simply by the decreasing N_2 percentage in the gasifying agent when CO_2 concentration increases. The concentration of N_2 reduced from 57.7% to 49.4%. Further, the Boudouard reaction shifting forward with rising CO_2 concentration can also explain the increase in CO concentration. At the identical CO_2/agent ratio variation, the CO concentration increased from 35.9% to 40.1%. In syngas, the CO_2 content (0.4%) is quite low. Even a ten percent CO_2 in the gasifying agent did not result in a significant volume of CO_2 gas. That instance, a ten percent CO_2 component in the gasifying agent appears to be environmentally friendly. Moreover, the H_2 concentration increased from 1.2% to 9.6% with the increase of the CO_2 fraction in the gasification agent. The forward shift of the dry reforming reaction with increasing CO_2 percentage provides the enhanced H_2 concentration. Similarly, the dry reforming process resulted in a decline in CH_4 concentration from 5.2% to 0%. In addition, at a CO_2/agent ratio of 7.5%, fraction change trends shift. There was a slowing of the rate of increase or decrease in the concentrations of the gas components. Hence, when considering the syngas composition, the optimal CO_2/agent ratio is 7.5%. The quantity of CO_2 in the gasifying agent has an impact on the system's efficiency, since it influences the syngas content and therefore its quality, as well as the amount of energy required by the compressor and reactor. Fig. 10 shows the variance in energetic and exergetic efficiency for individual and overall systems as a function of CO_2/agent ratio.

The gasifier's energy efficiency declined from 67.67% to 66.54%

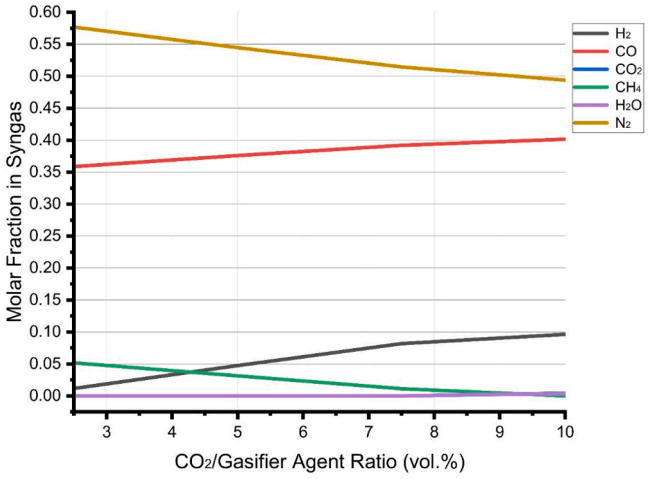

Fig. 9. Variation in gaseous component concentrations in syngas depending on the CO_2/agent ratio.

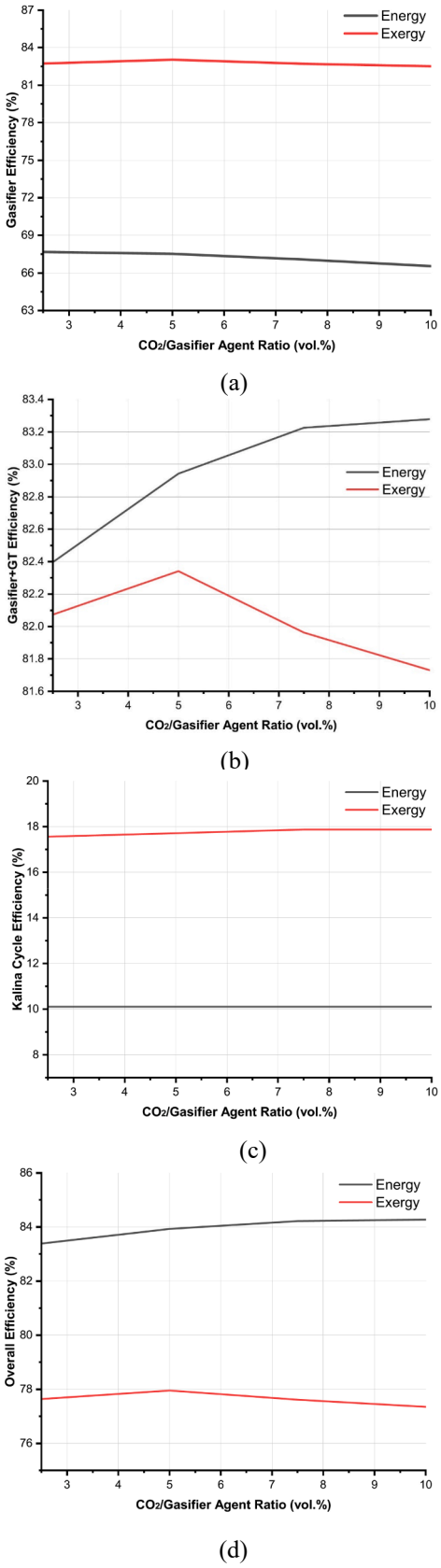

Fig. 10. The effect of the CO_2/agent ratio on the energetic and exergetic efficiency of individual systems and the overall system.

when the CO_2/agent ratio increased. Even though the quality of syngas improved as the amount of CO_2 supplied raised, the boosting of endothermic reactions and the growth in compressor power may have resulted in a decrease in efficiency. The exergetic efficiency, on the other hand, did not change significantly (reducing from 82.73% to 82.51%), although it did increase when the CO_2/agent ratio was elevated to 5%, and then decreased. While the energetic efficiency improved from 82.40% to 83.28% in the gasifier/GT system, the exergetic efficiency declined from 82.07% to 81.73%. Obtaining syngas at greater mass flow enhanced the amount of power generated in the GT, even if the auxiliary power for the equipment increased with the growth in CO_2 supply. When the CO_2/agent ratio was 7.5% and above, however, no significant improvement in energy efficiency was noticed. The exergetic efficiency of the gasifier/GT system increased until the CO_2/agent ratio reached 5%, then decreased, similar to the gasifier system. With rising CO_2 content in the gasifying agent, the Kalina cycle's energy efficiency remained almost unchanged. Exergetic efficiency, on the other hand, improved from 17.56% to 17.88%. Additionally, when the CO_2/agent ratio was 7.5% and higher, the exergetic efficiency did not change. Consequently, the overall system's energy efficiency improved from 83.39% to 84.28%, but the exergy efficiency declined from 77.64% to 77.35%. In conclusion, whereas a CO_2 concentration of 7.5% appears to be the optimum value for energy efficiency, a CO_2 concentration of 5% appears to be the optimum value for exergetic efficiency.

3.2.5. Effect of ammonia/water ratio

Since the ammonia–water mixture is a non-azeotropic working fluid, its boiling and condensing properties are diverse. Thermodynamic irreversibility is reduced by changing temperature during heat-transfer activities [73], which affects process efficiency. Therefore, modifying the ammonia proportion of the mixture impacts the efficiency of the Kalina cycle. Fig. 11 depicts the effect of ammonia concentration in the operational fluid on energetic and exergetic efficiency.

Due to ammonia's lower boiling point than water, the Kalina cycle's working fluid having a high ammonia proportion tends to evaporate to a higher extent under a fixed evaporation pressure and cooling condition. Thus, the working fluid's volume flow rate rises. As a result of the increased ammonia proportion in the working fluid, the turbine's work output rises. The energy efficiency of the Kalina cycle increased from 6.15% to 12.15% when the ammonia proportion was improved, while the overall cycle's energetic efficiency increased from 83.88% to 84.48%. Similarly, the exergetic efficiency of the Kalina cycle increased from 10.95% to 21.56% when the ammonia proportion was improved, while the overall cycle's energetic efficiency increased from 76.93% to 77.52%. Other studies have confirmed the correlation between the rising content of ammonia in the working fluid and the increment in power output and efficiency [74–76].

3.2.6. Effect of pressure before the Kalina turbine

Because of the varying turbine power generation, the influence of the Kalina turbine's inlet pressure is critical to the system's effectiveness. Fig. 12 illustrates the effect of Kalina turbine inlet pressure on energetic and exergetic performance.

Initially, as the working fluid expands further, the turbine's power output rises with the growth in turbine inlet pressure. The energy efficiency rises from 9.75% to 10.14% when the turbine inlet pressure is increased to 28 bar, and the exergetic efficiency rises from 17.32% to 18.03%. The efficiency of the Kalina cycle, on the other hand, rises to a particular threshold, peaks, and then declines. Beyond 28 bar, the process efficiency decreases; at 40 bar, the energetic efficiency drops to 9.39% and the exergetic efficiency drops to 16.66%. The features of the ammonia-water solution is used to understand the behavior behind this phenomenon. The boiling point of the ammonia-water mixture increases as pressure is increased. As a consequence, the liquid phase's volume in the two-phase fluid increases. Furthermore, the Kalina turbine's power generation is reduced as a result of this. Since streams with low

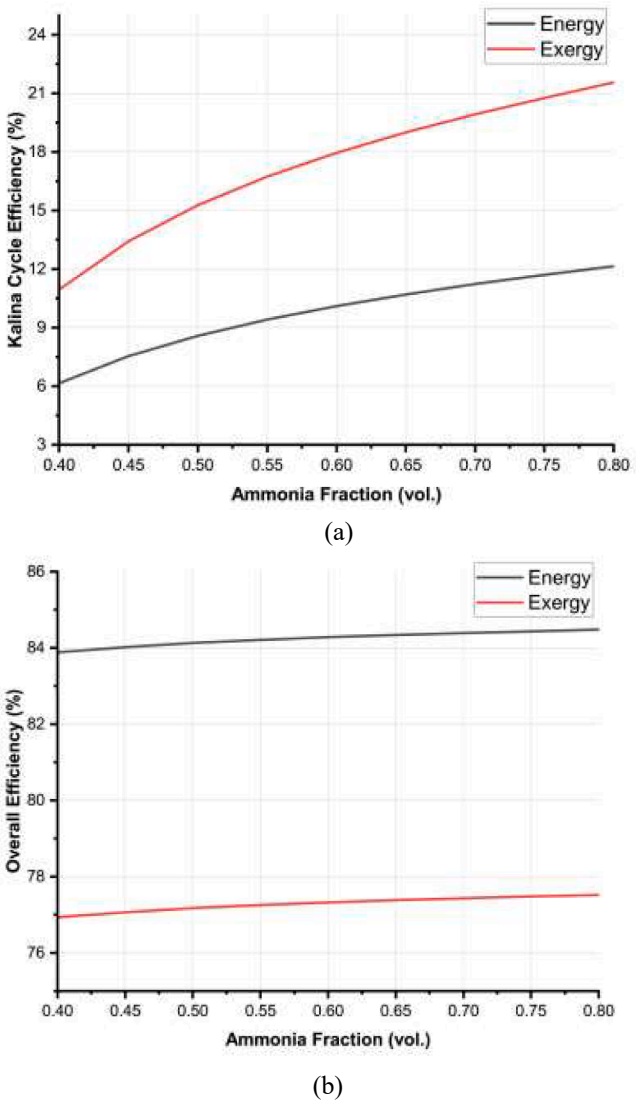

Fig. 11. The impact of the ammonia concentration on the energetic and exergetic efficiencies of the Kalina cycle and the overall system.

ammonia concentrations are cooler than working fluid, the temperature of the stream exiting the mixer changes as well. As a result, the temperatures of the heat exchanger's incoming and outgoing streams fluctuate, as does the temperature of the final syngas. The heat transferred to the Kalina cycle, and hence the system efficiency, is affected by this occurrence. Similar deductions have also been reported by Hossain et al. [77]. The energy and exergy efficiency of the overall system is identical to the Kalina cycle characteristic because the Kalina turbine inlet pressure has no influence on the gasifier or gasifier/GT system. At 28 bar, the overall system's energy efficiency increased to 84.29%, then declined to 84.21% at 40 bar. Further, when the pressure was raised to 28 bar, the exergy efficiency improved to 77.33%, then dropped to 77.28% when the pressure was raised to 40 bar.

3.2.7. Effect of pressure after the Kalina turbine

The pressure at which the working fluid expands is a crucial parameter since it affects the Kalina cycle and hence the integrated system's energy and exergy efficiencies. Fig. 13 demonstrates the effect of Kalina turbine outlet pressure on energetic and exergetic performance.

The energetic efficiency of the Kalina cycle declines from 10.51% to 6.93% when the Kalina turbine outlet pressure rises, whereas the

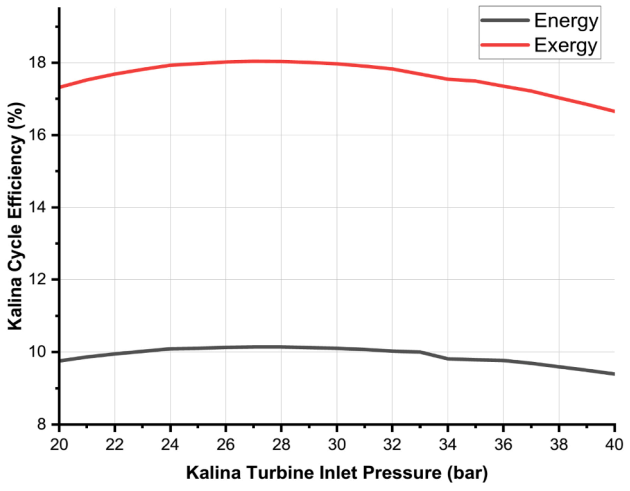

(a)

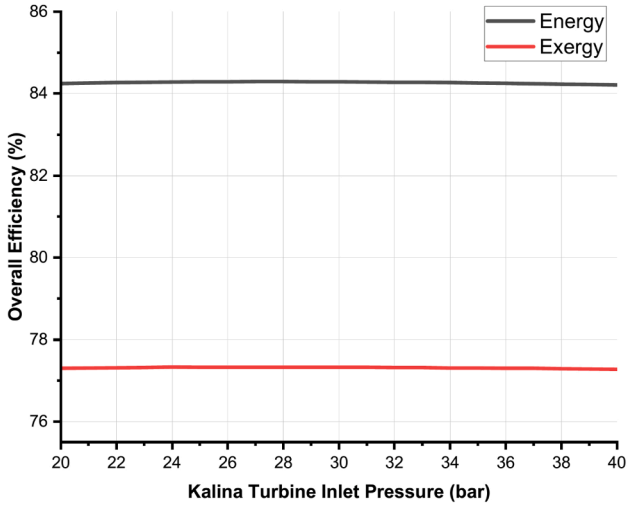

(b)

Fig. 12. The effect of the pressure at the inlet of the Kalina turbine on the energetic and exergetic efficiency of the Kalina cycle and the overall system.

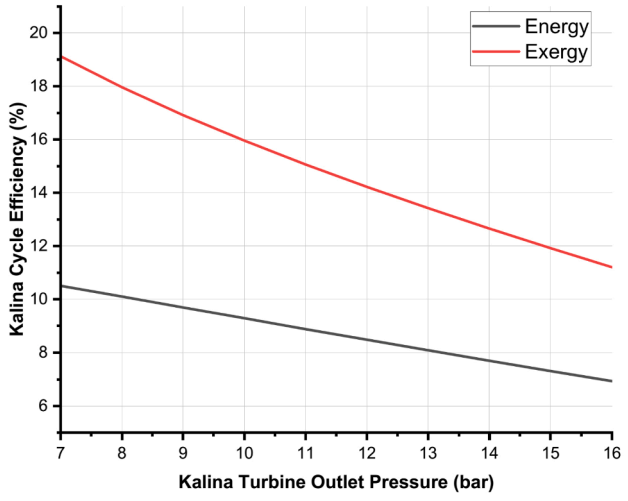

(a)

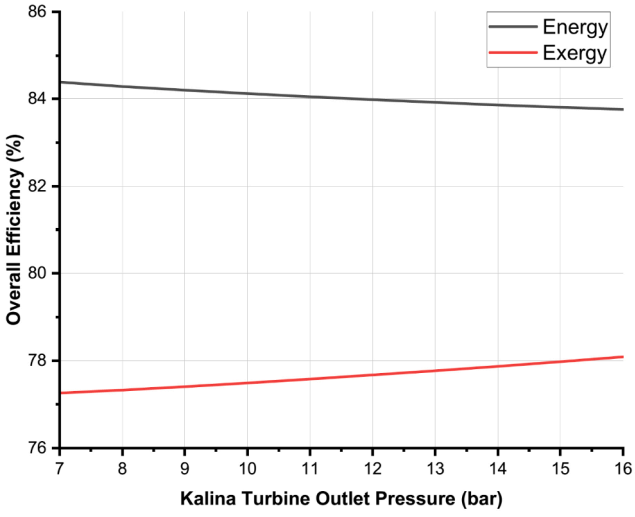

(b)

Fig. 13. The effect of the pressure at the outlet of the Kalina turbine on the energy and exergetic efficiency of the Kalina cycle and the overall system.

exergetic efficiency decreases from 19.13% to 11.20%. Although the power required to raise the working fluid to high pressures in order to attain operating pressure decreases, expanding to lower pressures improves the amount of power generated in the turbine considerably. The overall system's energy and exergy efficiency displayed different tendencies. Exergetic efficiency increased from 77.26% to 78.09%, whereas energetic efficiency decreased from 84.39% to 83.76%. Less exergy destruction resulted in lower energy efficiency.

The parametric analysis results indicate that ER is the most effective parameter among the gasifier system's operating conditions. The ER highly influences the syngas composition, flow rate of produced gases, chemical exergy of syngas, and energy/exergy efficiency of the gasifier and overall system. However, the Kalina cycle was more impacted by its own operating circumstances than the gasifier's. The composition of the working fluid, in particular, can affect the energy efficiency of the Kalina cycle by 6% and the exergy efficiency by 11%. The Kalina cycle's relatively low power, on the other hand, could not have a substantial impact on the overall system's energy/exergy efficiency.

3.3. Exergy flow analysis

In various applications, Sankey diagrams are used to visualize material and energy transfers, to help comprehension of losses and inefficiencies, to chart manufacturing operations, and to provide a notion of scale throughout a system [78]. In this study, the arrows represent inlet and outlet material streams (blue colored) and energy streams (dark red colored), rectangular boxes represent the main unit blocks (light red colored), and the width of the lines connecting the unit blocks (orange colored) was varied to visually represent the amount of exergy flow. The Sankey diagram of an integrated system in base condition is shown in Fig. 14.

The GT produces the majority of combined cycle power, which is equivalent to 1503 kW, while the entrained bed gasifier consumes the vast majority of combined cycle power, which is equal to 1074 kW. The disadvantageous condition generated by the power need for the endothermic gasification process is compensated for by converting syngas at high temperature and pressure to power in the GT before entering the Kalina cycle. When examining the auxiliary equipment, the amount of energy required for the pumps is quite minimal, however the amount of energy necessary for the compressor (489 kW) is substantial. In the

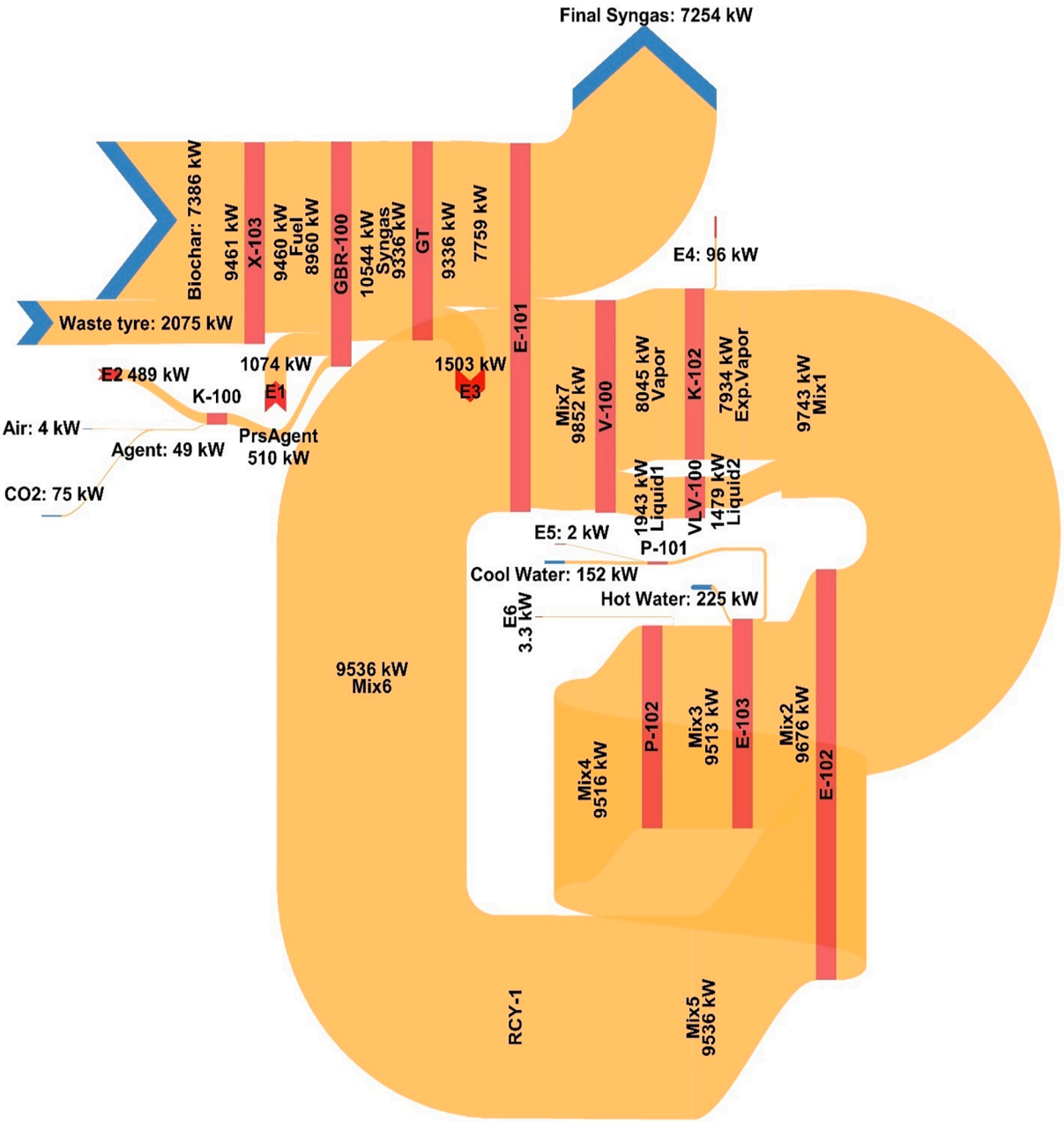

Fig. 14. Sankey diagram for the newly proposed entrained bed gasifier/GT/Kalina cycle system.

integrated system, the exergy flow of the feedstock material and the working fluid is equivalent. The feedstock material's exergy is solely chemical, whereas the working fluid's exergy is a combination of chemical and physical exergy. It is also worth mentioning that the working fluiding flow is around three times more than the feedstock flow. Moreover, the gasifier is the equipment that destroys the most exergy (1208 kW). When synthesizing product gas from solid fuel, there is a significant level of exergy loss.

4. Conclusion

In this work, a novel integrated system was developed and investigated that includes an entrained bed gasifier, a GT, and a Kalina cycle. The effectiveness of the integrated system was evaluated by analyzing not only the operational characteristics of the Kalina cycle, but also various process parameters of the entrained bed gasifier. Thus, several case studies were conducted to determine the optimal operating parameters, such as gasifier temperature, ER, feedstock and gasifying agent properties, ammonia-water mixture, and Kalina turbine inlet and outlet pressures to achieve optimal energy and exergy yields. Below are some of the main conclusions of the study:

- The optimum syngas composition seems to be achieved with the value of ER = 0.29. However, the best energetic efficiency was achieved at ER = 0.23, whereas the best exergetic efficiency was obtained at ER = 0.25.
- It was found that increasing the concentration of waste tyres in the feedstock improved H_2 production, while CO production decreased. Moreover, the N_2 concentration in the syngas decreases with increasing waste tyre content. Increasing the waste tyre content improves the energy efficiency of the overall system, while decreasing the exergy efficiency.
- Syngas composition was rather stable over gasifier temperature changes from 1300 to 1700 °C. On the other hand, the energy

efficiency of the overall system was impacted negatively by the high energy required for operation at high temperatures.

- The gasification agent content was found to be one of the most effective criteria. For optimal syngas composition and energy efficiency, a CO_2/agent ratio of 7.5% was determined. However, for exergetic efficiency, a CO_2/agent ratio of 5% was determined to be the most efficient.
- The working fluid with a high ammonia concentration performed better in terms of energy and exergy efficiency.
- The ideal value for the Kalina turbine inlet pressure was set at 28 bar. Energy efficiency improves at lower expansion pressures, whereas exergy efficiency decreases.
- The integration of a GT into the gasification system is critical for exergy recovery. In addition, determining the best gasifier operating settings is critical for ensuring the integrated system's efficiency since the gasifier is the piece of equipment where the greatest exergy destruction is calculated.

For low-temperature waste heat recovery, the Kalina cycle is often used because of the properties of its working fluid. Many Kalina cycle configurations, however, have been documented at a wide variety of heat source temperatures. Therefore, in this paper, energy and exergy analysis was carried out for the Kalina cycle system combined with the entrained bed gasifier, which is utilized for high-capacity gasification applications. However, a GT was utilized for pre-cooling and extra power generation rather than employing the syngas produced at high temperatures and high pressures directly as a heat source in the Kalina cycle. Thus, more power is produced without affecting the syngas composition, and a more suitable thermal source is provided for the Kalina cycle.

In this work, the gasification process was simulated in Aspen HYSYS from the feedstock material onwards, which is in contrast to the studies in the literature. Gasification or gasification-driven studies in the literature begin with pre-defined syngas properties since Aspen HYSYS lacks a comprehensive library for solid processing. In addition, in the parametric analyzes performed for integrated systems including Kalina cycle, Kalina cycle parameters are majorly evaluated, or only a few independent variables from other systems are considered. Energy and exergy analyses in this work, on the other hand, were performed by analyzing a wide range of gasification conditions, including solid fuel characteristics, in combination with Kalina cycle operating parameters. Consequently, not only can the overall system's performance be assessed, but also the performance of individual subsystems under a variety of operational settings, allowing for the determination of each subsystem's best operating condition.

Both the entrained bed gasification and Kalina cycle operations produced results that coheres with the scientific background and literature results in terms of the reactions that occurred, the physicochemical phenomena that were observed, and the energy and exergy performances that were found. Thus, in future studies, Aspen HYSYS simulator can be used as an alternative to Aspen Plus for solid fuel-driven processes. Studies to be carried out for the simulation of combined power generation cycles involving gasification can also be conducted by including the gasification phenomena. By providing the appropriate configurations for the integrated system simulation, thermodynamic analyzes can be performed, which can provide results consistent with the literature.

CRediT authorship contribution statement

Furkan Kartal: Data curation, Investigation, Software, Validation, Visualization, Writing – original draft, Writing – review & editing. **Uğur Özveren:** Conceptualization, Formal analysis, Funding acquisition, Methodology, Project administration, Resources, Supervision, Data curation, Investigation, Software, Validation, Visualization, Writing – original draft, Writing – review & editing.

Declaration of Competing Interest

The authors declare that they have no known competing financial interests or personal relationships that could have appeared to influence the work reported in this paper.

Data availability

Data will be made available on request.

Acknowledgement

This work has been supported by Marmara University Scientific Research Projects Coordination Unit under grant number FYL-2020-10139.

References

[1] Yilmaz F, Ozturk M, Selbas R. Design and thermodynamic analysis of coal-gasification assisted multigeneration system with hydrogen production and liquefaction. Energy Convers Manage 2019;186:229–40.
[2] Kavouridis K, Koukouzas N. Coal and sustainable energy supply challenges and barriers. Energy Policy 2008;36(2):693–703.
[3] Gent S, Twedt M, Gerometta C, Almberg E. Theoretical and applied aspects of biomass torrefaction: for biofuels and value-added products. Butterworth-Heinemann; 2017.
[4] Bonechi C, Consumi M, Donati A, Leone G, Magnani A, Tamasi G, et al. In: Biomass: an overview. Bioenergy systems for the future. Elsevier; 2017. p. 3–42.
[5] Anniwaer A, Chaihad N, Zahra ACA, Yu T, Kasai Y, Kongparakul S, et al. Steam co-gasification of Japanese cedarwood and its commercial biochar for hydrogen-rich gas production. Int J Hydrogen Energy 2021;46(70):34587–98.
[6] Tian H, Hu Q, Wang J, Chen D, Yang Y, Bridgwater AV. Kinetic study on the CO2 gasification of biochar derived from Miscanthus at different processing conditions. Energy 2021;217:119341.
[7] Martínez JD, Puy N, Murillo R, García T, Navarro MV, Mastral AM. Waste tyre pyrolysis–A review. Renew Sustain Energy Rev 2013;23:179–213.
[8] Gasification HC. Combustion engineering issues for solid fuel systems. Elsevier; 2008. p. 423–68.
[9] Ramos IAC, Montini T, Lorenzut B, Troiani H, Gennari FC, Graziani M, et al. Hydrogen production from ethanol steam reforming on M/CeO2/YSZ (M= Ru, Pd, Ag) nanocomposites. Catal Today 2012;180(1):96–104.
[10] Bhattacharya S, Kabir KB, Hein K. Dimethyl ether synthesis from Victorian brown coal through gasification–Current status, and research and development needs. Prog Energy Combust Sci 2013;39(6):577–605.
[11] Moreira R, Bimbela F, Gil-Lalaguna N, Sánchez JL, Portugal A. Clean syngas production by gasification of lignocellulosic char: state of the art and future prospects. J Ind Eng Chem 2021.
[12] Minchener AJ. Coal gasification for advanced power generation. Fuel 2005;84(17):2222–35.
[13] Dai B, Zhang L, Cui J-f, Hoadley A, Zhang L. Integration of pyrolysis and entrained-bed gasification for the production of chemicals from Victorian brown coal—Process simulation and exergy analysis. Fuel Process Technol 2017;155:21–31.
[14] Simbeck D, Korens N, Biasca F, Vejtasa S, Dickenson R. Coal gasification guidebook: status, applications, and technologies. Final report TR-102034 Electric Power Research Institute, Palo Alto. Calif 1993.
[15] Safronov D, Förster T, Schwitalla D, Nikrityuk P, Guhl S, Richter A, et al. Numerical study on entrained-flow gasification performance using combined slag model and experimental characterization of slag properties. Fuel Process Technol 2017;161:62–75.
[16] Tremel A, Becherer D, Fendt S, Gaderer M, Spliethoff H. Performance of entrained flow and fluidised bed biomass gasifiers on different scales. Energy Convers Manage 2013;69:95–106.
[17] van Dongen A, Kanaar M. Co-gasification at the Buggenum IGCC power plant. 2006.
[18] Font O, Cordoba P, Querol X, Coca P, Garcia-Peña F. Co-gasification of biomass: Effect on the fate of trace elements. World of Coal Ash Conference 2011:9–12.
[19] Dincer I. Environmental and sustainability aspects of hydrogen and fuel cell systems. Int J Energy Res 2007;31(1):29–55.
[20] Ordorica-Garcia G, Douglas P, Croiset E, Zheng L. Technoeconomic evaluation of IGCC power plants for CO2 avoidance. Energy Convers Manage 2006;47(15–16):2250–9.
[21] Frey HC, Zhu Y. Improved system integration for integrated gasification combined cycle (IGCC) systems. Environ Sci Technol 2006;40(5):1693–9.
[22] Okeily M, Mikhael N, Morad K, Mohamed AM. A Comparative Study of Integrated Coal Gasification Combined-Cycle Power Plants (ICGCC) with Kalina Cycle. Port-Said Eng Res J 2014;18(1):42–58.
[23] Dincer I, Demir ME. 4.8 Steam and Organic. Rankine Cycles 2018.
[24] Seckin C. Effect of Operational Parameters on a Novel Combined Cycle of Ejector Refrigeration Cycle and Kalina Cycle. J Energy Res Technol 2020;142(1).

[25] Wang E, Yu Z. A numerical analysis of a composition-adjustable Kalina cycle power plant for power generation from low-temperature geothermal sources. Appl Energy 2016;180:834–48.
[26] Rezaee V, Houshmand A. Energy and exergy analysis of a combined power generation system using PEM fuel cell and Kalina Cycle System 11. Periodica Polytech, Chem Eng 2016;60(2):98–105.
[27] Bombarda P, Invernizzi CM, Pietra C. Heat recovery from Diesel engines: A thermodynamic comparison between Kalina and ORC cycles. Appl Therm Eng 2010;30(2–3):212–9.
[28] Cao L, Wang J, Dai Y. Thermodynamic analysis of a biomass-fired Kalina cycle with regenerative heater. Energy 2014;77:760–70.
[29] Ojeda KA, Sánchez-Tuirán E, Gonzalez-Diaz J, Gomez-Ochoa M, Kafarov V. Exergy analysis applied to microalgae-based processes and products. In: Handbook of Microalgae-Based Processes and Products. Elsevier; 2020. p. 841–59.
[30] More P, Aijaz A. Thermal analysis of energy and exergy of back pressure steam turbine in sugar cogeneration plant. Int J Emerg Technol Adv Eng 2014;4(1):674–82.
[31] Ibrahim Dincer MAR. Exergy and energy analyses. EXERGY - Energy: Environment and Sustainable Development; 2007. p. 23–5.
[32] Ertesvåg IS. Exergetic comparison of efficiency indicators for combined heat and power (CHP). Energy 2007;32(11):2038–50.
[33] Dong K, Rong Q, Li M, Lin J, Xiao R, Li Y. A novel simulation for gasification of Shenmu Coal in an entrained flow gasifier. Chem Eng Res Des 2020;160:454–64.
[34] Pierobon L, Rokni M. Thermodynamic analysis of an integrated gasification solid oxide fuel cell plant with a Kalina cycle. IJGE 2015;12(6):610–9.
[35] Ji-chao Y, Sobhani B. Integration of biomass gasification with a supercritical CO2 and Kalina cycles in a combined heating and power system: A thermodynamic and exergoeconomic analysis. Energy 2021;222:119980.
[36] Zoghi M, Habibi H, Chitsaz A, Holagh SG. Multi-criteria analysis of a novel biomass-driven multi-generation system including combined cycle power plant integrated with a modified Kalina-LNG subsystem employing thermoelectric generator and PEM electrolyzer. Therm Sci Eng Prog 2021;26:101092.
[37] Tan L, Dong X, Gong Z, Wang M. Investigation on performance of an integrated SOFC-GE-KC power generation system using gaseous fuel from biomass gasification. Renewable Energy 2017;107:448–61.
[38] Safder U, Nguyen H-T, Ifaei P, Yoo C. Energetic, economic, exergetic, and exergorisk (4E) analyses of a novel multi-generation energy system assisted with bagasse-biomass gasifier and multi-effect desalination unit. Energy 2021;219:119638.
[39] Yan L, Yue G, He B. Thermodynamic analyses of a biomass–coal co-gasification power generation system. Bioresour Technol 2016;205:133–41.
[40] Ersöz A, DurakÇetin Y, Sarıoğlan A, Turan A, Mert M, Yüksel F, et al. Investigation of a novel & integrated simulation model for hydrogen production from lignocellulosic biomass. Int J Hydrogen Energy 2018;43(2):1081–93.
[41] Tauqir W, Zubair M, Nazir H. Parametric analysis of a steady state equilibrium-based biomass gasification model for syngas and biochar production and heat generation. Energy Convers Manage 2019;199:111954.
[42] Zang G, Tejasvi S, Ratner A, Lora ES. A comparative study of biomass integrated gasification combined cycle power systems: Performance analysis. Bioresour Technol 2018;255:246–56.
[43] Burulday ME, Mert MS, Javani N. Thermodynamic analysis of a parabolic trough solar power plant integrated with a biomass-based hydrogen production system. Int J Hydrogen Energy 2022;47(45):19481–501.
[44] Roddy DJ, Manson-Whitton C. Biomass Gasification and Pyrolysis. Comprehensive Renewable Energy, Vol 5: Biomass and Biofuel. Production 2012:133–53.
[45] Knoef H. Handbook Biomass Gasification. The Netherlands: BTG Biomass Technology Group; 2005.
[46] Liu S, Xing Y, Chen H, Tang P, Jiang J, Tang S, et al. Sustainable Reactors for Biomass Conversion Using Pyrolysis and Fermentation. 2017.
[47] Wang W, Wen C, Liu T, Li C, Liu H, Liu E, et al. Emissions of PM10 from the co-combustion of high-Ca pyrolyzed biochar and high-Si coal under air and oxyfuel atmosphere. P Combust Inst 2021;38(3):4091–9.
[48] Zhang J-l, Shan R, Su B-x. Lin Y-h, Long S-g. Combustion ratio of waste tire particle, PC and mixture at blast temperature of BF. J Iron Steel Res Int 2012;19(2):12–6.
[49] Emun F, Gadalla M, Majozi T, Boer D. Integrated gasification combined cycle (IGCC) process simulation and optimization. Comput Chem Eng 2010;34(3):331–8.
[50] Preciado JE, Ortiz-Martinez JJ, Gonzalez-Rivera JC, Sierra-Ramirez R, Gordillo G. Simulation of synthesis gas production from steam oxygen gasification of Colombian coal using Aspen Plus®. Energies 2012;5(12):4924–40.
[51] Faraji M, Saidi M. Hydrogen-rich syngas production via integrated configuration of pyrolysis and air gasification processes of various algal biomass: Process simulation and evaluation using Aspen Plus software. Int J Hydrogen Energy 2021;46(36):18844–56.
[52] Salisu J, Gao N, Quan C. Techno-economic assessment of co-gasification of rice husk and plastic waste as off-grid power source for small scale rice milling in nigeria-an aspen plus model. J Anal Appl Pyrol 2021;105157.
[53] Dimian AC, Bildea CS, Kiss AA. Process Synthesis by the Hierarchical Approach. Elsevier Comput Aided Chem Eng 2014:253–300.
[54] Lwin Y. Chemical equilibrium by Gibbs energy minimization on spreadsheets. Int J Eng Educ 2000;16(4):335–9.
[55] Bejan A, Tsatsaronis G, Moran MJ. Thermal design and optimization. John Wiley & Sons; 1995.
[56] Tsatsaronis G. Definitions and nomenclature in exergy analysis and exergoeconomics. Energy 2007;32(4):249–53.
[57] Kotas TJ. The exergy method of thermal plant analysis. Elsevier; 2013.
[58] Saidur R, BoroumandJazi G, Mekhilef S, Mohammed H. A review on exergy analysis of biomass based fuels. Renew Sust Energ Rev 2012;16(2):1217–22.
[59] Szargut J, Styrylska T. Approximate evaluation of the exergy of fuels. Brennst Wärme Kraft 1964;16(12):589–96.
[60] Weiland F, Hedman H, Marklund M, Wiinikka H, Öhrman O, Gebart R. Pressurized oxygen blown entrained-flow gasification of wood powder. Energy Fuels 2013;27(2):932–41.
[61] Yun Y, Yoo YD, Chung SW. Selection of IGCC candidate coals by pilot-scale gasifier operation. Fuel Process Technol 2007;88(2):107–16.
[62] Lee J-W, Yun Y, Chung S-W, Kang S-H, Ryu J-H, Kim G-T, et al. Application of multiple swirl burners in pilot-scale entrained bed gasifier for short residence time. Fuel 2014;117:1052–60.
[63] Agraniotis M, Bergins C, Stein-Cichoszewska M, Kakaras E. High-efficiency pulverized coal power generation using low-rank coals. Low-Rank Coals for Power Generation. Fuel and Chemical Production Elsevier 2017:95–124.
[64] Li S, Dai Y. Thermo-economic comparison of Kalina and CO2 transcritical power cycle for low temperature geothermal sources in China. Appl Therm Eng 2014;70(1):139–52.
[65] Scala F. Fluidized bed technologies for near-zero emission combustion and gasification. Elsevier; 2013.
[66] Narvaez I, Orio A, Aznar MP, Corella J. Biomass gasification with air in an atmospheric bubbling fluidized bed. Effect of six operational variables on the quality of the produced raw gas. Ind Eng Chem Res 1996;35(7):2110–20.
[67] Zang G, Jia J, Shi Y, Sharma T, Ratner A. Modeling and economic analysis of waste tire gasification in fluidized and fixed bed gasifiers. Waste Manage 2019;89:201–11.
[68] Singh OK, Kaushik S. Energy and exergy analysis and optimization of Kalina cycle coupled with a coal fired steam power plant. Appl Therm Eng 2013;51(1–2):787–800.
[69] Basu P. Biomass characteristics: biomass gasification and pyrolysis. Nueva York: Oxford-Elsevier; 2010.
[70] Timsina R, Thapa RK, Moldestad BM, Eikeland MS. Computational particle fluid dynamics simulation of biomass gasification in an entrained flow gasifier. Chem Eng Sci: X 2021;12:100112.
[71] Lee JG, Kim JH, Lee HJ, Park TJ, Kim SD. Characteristics of entrained flow coal gasification in a drop tube reactor. Fuel 1996;75(9):1035–42.
[72] Shen Y, Li X, Yao Z, Cui X, Wang C-H. CO2 gasification of woody biomass: Experimental study from a lab-scale reactor to a small-scale autothermal gasifier. Energy 2019;170:497–506.
[73] Zhang X, He M, Zhang Y. A review of research on the Kalina cycle. Renew Sustain Energy Rev 2012;16(7):5309–18.
[74] Hossain MM, Hossain MS, Ahmed NA, Ehsan MM. Numerical Investigation of a modified Kalina cycle system for high-temperature application and genetic algorithm based optimization of the multi-phase expander's inlet condition. Energy and AI 2021;6:100117.
[75] Fan G, Dai Y. Thermo-economic optimization and part-load analysis of the combined supercritical CO2 and Kalina cycle. Energy Convers Manage 2021;245:114572.
[76] Zheng S, Chen K, Du Y, Fan G, Dai Y, Zhao P, et al. Comparative analysis on off-design performance of a novel parallel dual-pressure Kalina cycle for low-grade heat utilization. Energy Convers Manage 2021;234:113912.
[77] Hossain MM, Ahmed NA, Shahriyar MA, Ehsan MM, Riaz F, Salehin S, et al. Analysis and optimization of a modified Kalina cycle system for low-grade heat utilization. Energy Convers Manage: X 2021;12:100121.
[78] Lupton RC, Allwood JM. Hybrid Sankey diagrams: Visual analysis of multidimensional data for understanding resource use. Resour Conserv Recycl 2017;124:141–51.